Massachusetts Institute of Technology

Department of Civil and Environmental Engineering

Energy Storage in Conductive Carbon-Cement Composites

Author: Traian Nîrca

École Supérieure de Physique et de Chimie Industrielles de la Ville de Paris

supervised by:

Thibaut Divoux
Nicolas Chanut
Roland Pellenq

referent professor:
Annie Colin

November 2019

Contents

Acknowledgements

First of all I would like to thank Thibaut DIVOUX and Nicolas CHANUT for guiding me throughout the entirety of this project and being always available to sort out any question or problem. The weekly meetings and discussions we had were extremely useful for developing my scientific practice and knowledge. Your rigor, your investment and your passion for science are truly inspiring and I am hoping that I will be able to work with you again sometime in the future.

Secondly, I would want to thank the UMI and specifically Roland PELLENQ for the financial and administrative support that made this project possible. Your scientific contributions to this project were invaluable, while your openly humorous, but methodical personality set an example for all of us.

I would also like to thank Annie COLIN, Veronique BELLOSTA and the entire team of dean of studies at ESPCI, as well as Fonds ESPCI for allowing this project and helping me throughout the whole year. Without your support, this dream of mine would have not been possible.

A special thank you to Prof. Franz-Josef ULM and Prof. Gareth H. McKINLEY who allowed me to assist at their lectures and greatly broaden my horizons. Thank you to Stephen RUDOLPH for letting us use the machine shop and helping us design and machine new parts and setups. A special thank you to Yunguang ZHU for aiding us with capacitance measurements and allowing us to freely use his equipment. I would also like to thank Renal BACKOV and Nancy SOLIMAN for your scientific, but also personal contributions to this project. Our discussions greatly impacted the outcome of the project and your personal advices were always welcomed and highly appreciated. I wish you both good luck in your works!

A big thank you goes to Sama TAHA, Vincent DEMAN and Estelle SCHURER who made the lab work less dull, shared laughs, but also tasks and results with me. An important mention goes to Chelsea WATANABE and Magreth KAKOKO who helped me with many measurements. Thank you to Alix DUPIRE, Fadhel EL MAY and Alexis GERVAIX for being the best roommates and amazing friends that I will always miss a lot. I would like to thank Michela GERI, Bavand KESHAVARZ and Sami YAMANI for all the scientific discussions, for the great moments and for treating me like family this whole year. Last, but not least, I would like to thank my parents, Valentina and Nicolae NIRCA, who, although far away, were always close and supported my in all my endeavours.

Chapter 1

Introduction

1.1 Motivation

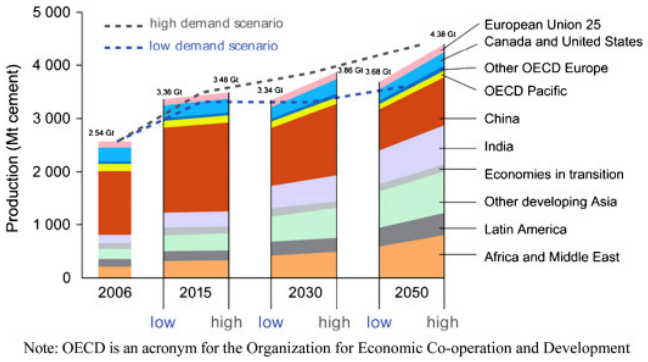

Figure 1.1: Annual world cement production. Reproduced from [1]. Even the lowest estimates suggest that by 2050 the annual production of cement will be 40% higher than in 2006. China is currently the world's largest importer of cement materials. Together with India and other countries in Asia, they are set to own more than 60% of the world's cement imports, by 2050.

Climate change is a pressing global problem that will have irreversible consequences on human activity and life in the following decades. Among the important actors contributing to climate change, cement industry plays an important role [2, 3]. It is estimated that about 6 to 10% of global carbon dioxide (CO_2) emissions come from Portland cement production, since one ton of cement produces approximately 0.9 tons of CO_2 [4, 5]. In the meantime, the cement production and consumption has been increasing in the last decades and keeps increasing: the annual production of cement in 2050 is expected to be double its level in 2006, as seen in Figure 1.1. There are many ways to positively impact the cement industry in order to reduce its environmental footprint: complete redesign of the production process, use of alternative raw materials, CO_2 capturing techniques or concrete reinforcement [1]. In our research, we are focusing on adding new functionalities to cement.

1.2 What is cement?

Cement is the product of the reaction between water and cement powder. The most common cement is the Portland cement, which is a hydraulic cement, whose main component is clinker, a mix of different proportions of calcium silicates. This powder is obtained through to the clinkering reaction, by heating limestone and clay in a rotary kiln to 1500°C (Fig. 1.2). The reaction is complex and has a lot of products, the most important ones being: calcium oxide (CaO), abbreviated as C, which is a product of the decalcination process of limestone, and silicon dioxide or silica (SiO_2), abbreviated as S, contained in clay [Fig. 1.3(a)] [6]. The clinkering reaction leads to the formation, among other components, of different calcium silicates like alite $(CaO)_3SiO_2$ (C_3S) or belite $(CaO)_2SiO_2$ (C_2S) that are called clinker. In contact with water (abbreviated as H), clinker dissolves, forming a colloidal suspension of hydration products when the solution becomes over saturated in free calcium.

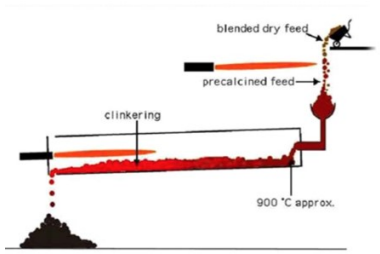

Figure 1.2: Principle of work of modern dry process kilns. Reproduced from [7].

The main products of hydration are calcium hydroxide $Ca(OH)_2$, called Portlandite, and calcium silica hydrates C-S-H [Fig. 1.3(b)]. The colloids also absorb water, different from the structural water included in the C-S-H group, effectively forming a gel, the cement paste. As the hydration goes on, the colloids grow and precipitate until reaching a percolation threshold. As the reaction advances, cement hardens, becoming a solid material. Hardened cement paste is a porous material, and the porosity is controlled by the water to cement ration (w/c), the ratio between water and cement powder initially used to make the cement paste [8]. The hydration of the clinker that creates several products, makes the cement a composite material. The main phases are Portlandite as discussed previously, and phases of calcium-silica-hydrates with different densities, depending on their local packing fraction in the hardened cement paste. Commonly, we make the distinction between the low density C-S-H phase and the high density C-S-H phase [9].

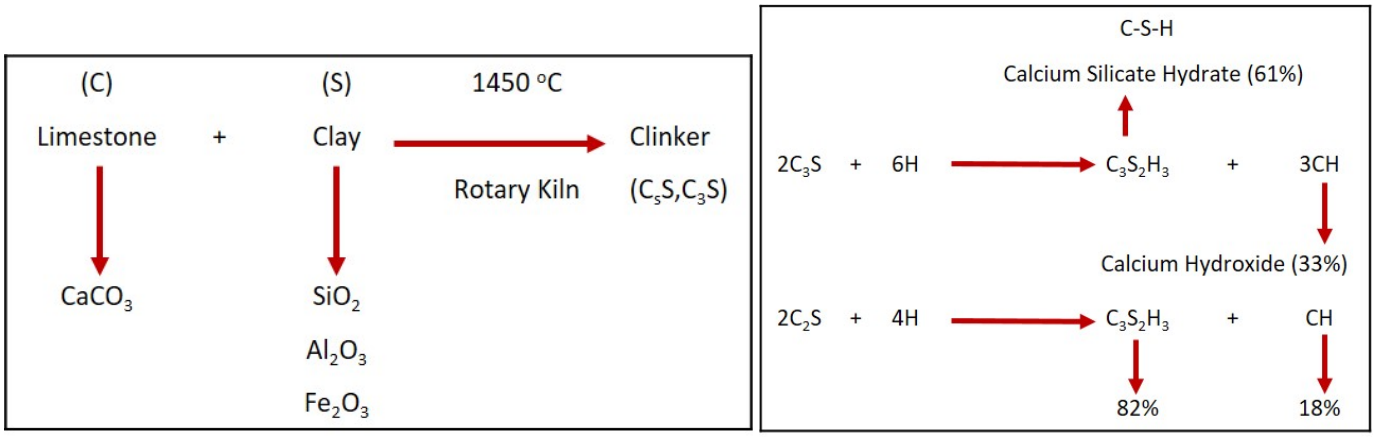

(a) (b)

Figure 1.3: (a) Clinkering reaction: formation of cement. Alite (C_3S) and belite (C_2S) are the main phases of clinker that participate in the hydration reaction. (b) Cement hydration and formation of calcium silicate hydrates.

1.3 Objective

Cement is an indispensable material for our society, yet it only plays an active role during the process of hydration and casting, being passive and inert throughout the rest of its lifespan. But what if we could give it a functionality and transform it into a material with a continuously added value ? Hardened cement paste is a highly porous material. Recent studies have found out that about 95% of its pores are interconnected [9], which means that they can potentially be used for ion storage. Using hardened cement paste to store energy in form of ions is a great way to enhance cement's functionality, but there is a problem. Doing it by using only cement might prove very challenging (or impossible), since cement is an insulator material. We decided to use cement and a conductive material, carbon black, in order to create an electrically conductive composite. In our research, we use cement as a dispersing matrix and carbon black as a dopant. Carbon black is a highly porous, conductive substance, whose nodules can assemble into bigger aggregate and agglomerates that can go up to hundreds of micrometers in diameter [10]. Its conductivity and porosity properties are very important, as it would allow the flow of electrons through the composite as well as the storage of ions. Moreover, compared to other carbonaceous substances, like carbon nanotubes or carbon fibers,

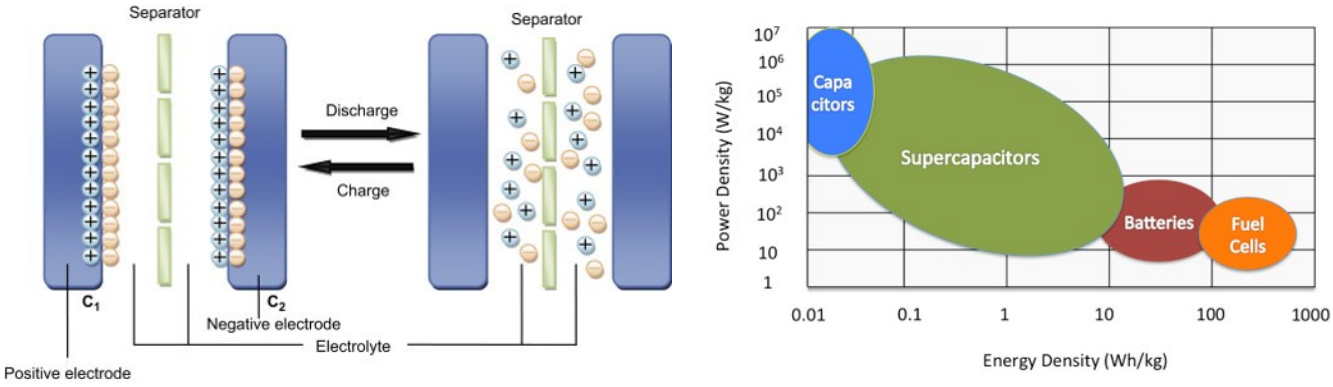

(a) Principle of a supercapacitor

(b) Power vs. energy density of energy storage devices

Figure 1.4: (a) Charge and discharge of a supercapacitor. Reproduced from [11]. (b) Performance of supercapacitors compared to other energy storage devices. A high power density means a fast charge-discharge rate, while a high energy density means a bigger amount of energy stored. Reproduced from [12].

carbon black is a relatively cheap material.

Driven by an environmental need, this project's ultimate goal is to construct energy storage devices using cement carbon composite. The envisioned device is called a supercapacitor. A supercapacitor is an electronic device, similar to a capacitor, that can store and release huge amounts of energy in a very short period of time. Where a capacitor uses a dielectric between two conductive plates, a supercapacitor uses an electrolyte and a separator between its plates, that is permeable to the ions but not to the electrons [Fig. 1.4(a)]. When a current is applied, the two plates are charged negatively and positively and the ions from the electrolyte are attracted to the plates: the supercapacitor is charged [11]. Its design allows supercapacitors to have a high power output compared to batteries, very high energy density compared to capacitors, as well as short charging rates and a long lifespan [Fig. 1.4(b)] [12]. This is achieved due to the separation of charge at the interface between the surface of the conductive electrode and the electrolyte. The separation of charge is of the order of a few ångströms, much smaller than in a conventional capacitor, which gives supercapacitors high specific capacitances and fast charge/discharge rates [13]. The first step of our research is to use the porous structure of cement as a medium to disperse carbon black, thus making the cement conductive. Once it is conductive, the goal is to use this cement to make electrodes and create a supercapacitor.

Our study is one of exploration, optimization and proof of concept. The first step of our approach is to demonstrate that our devices work efficiently on a small scale. To achieve this, we will explore the use of several carbon types, build carbon-cement electrodes and measure their resistivities and capacitance values. Once the first phase is complete and the suitable materials are selected, a scale up process will be initiated. The final goal of the project is to patent the results and collaborate with the industry in order to build structures or buildings, whose walls are, in fact, cement supercapacitors capable of storing electric energy.

1.4 Overview

Making conductive cement has been explored in various studies as early as the 1980s. In this section we will describe some of the works and patents already established for conductive concrete and their applications.

Conventional concrete, consisting of hydrated Portland cement with silica sand as fine aggregate and limestone, stone or other coarse aggregate, is a good electrical insulator. The electrical

resistivity of concrete usually ranges from 6.5 to 11.4 kΩ.m for dried concrete and 2.5 to 4.5 kΩ.m for moist concrete [14]. There are several uses, for a concrete that is electrically conductive. One of these uses is electromagnetic shielding [15]. It is often required in the design and construction of facilities and equipment to protect electrical systems or electronic components from the effects of unwanted electromagnetic energy. Other applications are radiation shielding in the nuclear industry; antistatic flooring in the electronic instrumentation industry and hospitals, cathodic protection of steel reinforcement in concrete structures, hydrophobic protection of roads, as well as Joule heating and other electronic applications [16, 17, 18].

These needs have been recognized for a number of years and some conductive concrete compositions and articles have been described in the technical and patent literature. In [16] Banthia *et al.*, studied the electrical resistivity of carbon fiber and steel micro-fiber reinforced cements. The content of conductive fiber ranged from 1 to 5% by volume. The resistivity at 28 days of hydration ranged from 78 to 32 kΩ.cm. Kojima *et al.*, in [19], prepared a highly conductive carbon fiber/cement composite by laminating sheets of carbon fiber paper impregnated with Portland cement paste. The product had a resistivity value of 0.7 Ω.cm. The material was highly effective in electromagnetic shielding, but very expensive and not suitable for load-bearing applications. Chiou *et al.*, in [18], reported work on carbon fiber reinforced cement for electromagnetic shielding, with results resembling those of [16]. Akira *et al.*, describes fiber-reinforced conductive concrete, useful for anti-static flooring, as comprising conductive fibers, reinforcement fibers, cement aggregates and synthetic resins or rubbers. They obtained a test piece having resistivity 1.8 MΩ.cm. Toshio *et al.*, describe electro-conductive cement compositions containing acetylene black. Mortar prepared from Portland cement, sand, partially oxidized acetylene black and water gave concrete having electrical resistance of 25 Ω one year after curing, and flexural and compressive strengths 43 and 190 kg.cm^{-2}, respectively.

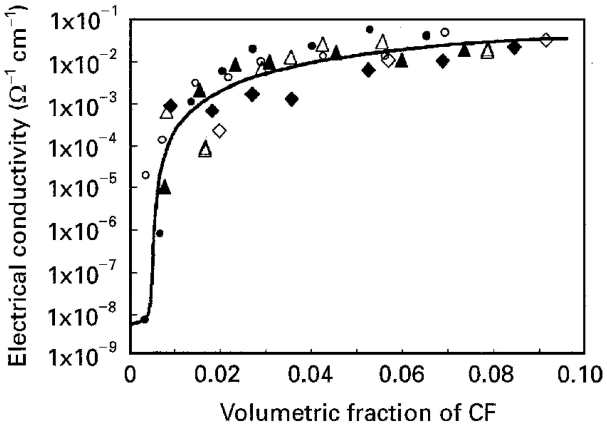

Figure 1.5: Conductivity versus carbon fibre content for paste systems. Water-cement ratio (w/c): filled diamond - 0.25, blank diamond - 0.30, filled triangle - 0.35, blank triangle - 0.40, filled circle - 0.45, blank circle - 0.50. Carbon fibre length = 3 mm. Reproduced from [20].

On a more theoretical approach, Xie *et al.* described in [20] the conductivity of cement-based composites with carbon fiber by a percolation model. They discovered that a minimum amount of carbon fiber was required to obtain a conductive composite and this amount depended on the size of the carbon fiber (Figure 1.5). They reached values as high as 0.05 S.cm^{-1} at volumetric fractions between cement and carbon fiber of 0.07. Tumijanski *et al.* points out in [21] that the mortar electrical behaviour appears to involve a competition between insulating aggregates, which lower the mortar's electrical conductivity and the development of transition zones between the paste and the aggregate which increases conductivity.

It should be noted that a compromise between high mechanical strength and relatively low electrical resistivity has not been achieved by any of the subject compositions. Many of the prior state of the art conductive concretes use a significant amount of carbon fiber which is relatively expensive. Accordingly, there is still a need for low-cost conductive concrete compositions combining good mechanical strength and high electrical conductivity.

More recently, Konsta-Gdoutos *et al.* showed that reinforcing cement with carbon nanotubes can greatly increase the strength of the materials, reporting a 25% increase in the mortar's flexural strength, with a peak of the distribution of the nanoindentation modulus in the area of 20–25 GPa, which represents the high stiffness C–S–H [22, 23]. Wen *et al.* report achieved resistivities in between 1 and 20 Ω.m for cement mixed with carbon fiber and carbon black, while maintaining decent mechan-

ical properties [24]. Sassani *et al*. studied the electrical conductivity of concrete to determine the optimum carbon fiber dosage for building heated pavement systems [25]. They determined that the optimum carbon fiber dosage was around 0.75-1% of volume for paste, mortar and concrete (Figure 1.6). However, the electrical conductivity of their system decreased dramatically with age, stabilizing after 150 days. They reached values of 0.012 S.cm^{-1} at 460 days. Kim *et al*. argue in [26] that the addition of small amounts of silica fume to the cement matrix contributes to a better dispersion of carbon nanotubes. This in turn results in an increase in compressive strength and the decrease in electrical resistance of carbon nanotube/cement composites.

Our goal is to synthesize samples with the lowest possible resistivity, but stable enough for capacitance measurements. This study had as a backbone the results of Pauline Genoud, an intern from ESPCI, who studied the mechanical properties and conductivity of carbon/cement/cellulose samples during a 3-month summer internship [27].

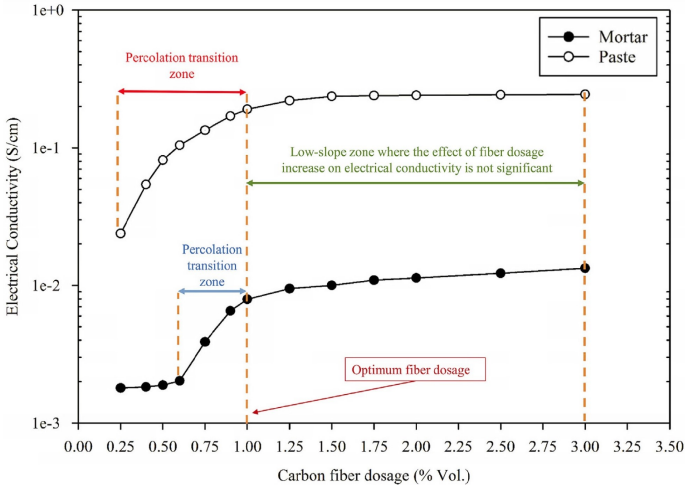

Figure 1.6: Variation of electrical conductivity by fiber content in cementitious paste and mortar. Reproduced from [25].

Chapter 2

Experimental Section

2.1 Synthesis of carbon-cement composites

The synthesis of the carbon-cement composites is achieved through mixing of cement, carbon and deionized water (DI). We synthesized and studied samples at three water to cement ratios (w/c): 0.42, 0.6 and 0.8, containing carbon ranging from 0 to 12% of total weight. For example, a typical sample at 11% carbon would contain 37.50 g of cement, 30 g of water and 8.40 g of carbon, with a w/c of 0.8. The procedure runs as follows:

1. The appropriate amount of cement and carbon powders are weighted using a high precision balance, OHAUS AX224, with a precision of 0.1 mg. Due to possible transfers of materials between containers, we do not go to higher precisions than the first two digits beyond zero (10 mg). The weighted material is placed into a plastic beaker.

2. The two powders are mixed in a Heidolph RZR 2102 electronic stirrer until a homogeneous dark grey powder is obtained, which usually takes between one and two minutes.

3. Under continuing mixing, the appropriate amount of DI water is gradually poured into the beaker. The mixing is not stopped until a homogeneous dark/black paste is obtained. This process can take up to ten minutes.

4. When the paste is ready, the mix is poured into cylindrical molds 7cm in length and 2.2cm interior diameter. A very viscous paste often requires being pushed or the cylinder being gently hit on a hard surface in a periodic manner for the composite to settle.

5. The cylinders are sealed on both sides with parafilm and placed in a saturated calcium hydroxide solution for 7 days.

The calcium hydroxide solution is used for two reasons: thermo-regulation and calcium source. Thermo-regulation is carried out by water, which homogenizes the temperature inside the samples, thus preventing the formation of cracks due to the build up of stresses, as well as slowing down the reaction, which leads to one that is more complete [28]. Although the samples are in molds and are not supposed to come in direct contact with the solution, the role of $Ca(OH)_2$ is to bring calcium ions and fill the cracks in the event of a breach. Cement becomes solid in a matter of hours, but the hydration reaction is not complete for weeks or months, which means that the properties of cement can still evolve. The age of the samples is recorded for every performed experiment and when comparing samples, we strive to do it at fixed dates: 14 days, 28 days, etc., in order to avoid the error due to ageing.

In order to convey new properties to our composites or improve on the existing ones, we have studied the influence of additives. When some form of additive is used, the steps 1-3 are replaced by a different protocol:

1. The appropriate amounts of additive (cellulose, potassium sulfate) and water are put together in a beaker, sealed, to prevent water evaporation and magnetically stirred for several hours or until the agent is completely dissolved in water.

2. The appropriate amount of carbon particles is added to the mix, the jar is once again sealed and left under magnetic stirring until the carbon is fully dispersed in the solution (typically 24h).

3. The carbon ink is mixed with the appropriate amount of cement in a plastic beaker and the two are mixed with an electric mixer until a homogeneous paste is obtained (typically up to ten minutes).

   The synthesis is continued with steps 4 and 5 of the original protocol.

In the case where surfactants are used to affect the viscosity and workability of the mixture, the appropriate amounts are added during step 3 of the original protocol, or at steps 1-2 of the dispersant protocol.

2.2 Sample preparation

After 7 days, the hardened samples are taken out of the calcium hydroxide bath and are left to dry at room temperature for several hours. The samples are taken out of their plastic molds using a press, yielding cylindrical samples with a length of roughly 6.5-7 cm and a diameter of 2.2 cm. These are in turn cut into smaller samples by using a diamond blade saw. Samples cut radially into sizes appropriate to the measurements performed on them: 0.6-2.5 cm in thickness for resistivity measurements and 0.1-0.7 cm in thickness for capacitance measurements.

Once cut, the samples are both rough and uneven, having non-parallel surfaces on the top and bottom sides. To ensure a good contact with the electrodes, these top and bottom surface of the samples must be parallel and polished. Both are achieved by polishing using silicium carbyde grinding papers at different grits: 120 and 220 to make the sample parallel, then gradually 400, 600, 1000, 1200 and 4000 grits (ranging from 110μm to 5μm) until a mirror like effect is achieved. Obtaining a well polished sample is not easy and is a very tedious task, but if made right, it can save time by eliminating the necessity of repeating the polishing (as well as the experiments) and minimizing the errors due to imperfect contact between the measuring electrodes and the sample surface.

Once polished, the samples made for resistivity measurements are ready, whereas those used for capacitance measurements require an additional treatment. For capacitance measurements, we sandwich a circular piece of glassy fiber with two carbon-cement electrodes (cf. §2.3.3). Thus, two samples are required for one capacitance measurement. After polishing, the samples are put inside in small jar and immersed in a 1 M potassium chloride solution. To ensure the samples are completely soaked, they are kept in the solution and under partial vacuum for 2-3 hours prior to the measurements.

2.3 Techniques for sample characterization

2.3.1 Scanning Electron Microscopy

A Scanning Electron Microscope, or SEM, is an electron microscope that produces images of a sample by scanning the surface with a focused beam of electrons. The electrons interact with atoms in the sample, producing signals that contain information about the surface topography and composition of the sample [29]. The electron beam is scanned in a raster scan pattern, and the position of the beam is combined with the intensity of the detected signal to produce an image. Secondary electrons emitted by atoms excited by the electron beam are captured by a detector. The number of secondary electrons that can be detected, and thus the signal intensity, depends on the specimen topography. A SEM can achieve a resolution as low as one nanometer. SEM samples have to be small enough to fit on the specimen stage, and may need special preparation to increase their electrical conductivity and to stabilize them, so that they can withstand the high vacuum conditions and the high energy beam of electrons. Samples are generally mounted rigidly on a specimen holder or stub using a conductive adhesive [30].

Nonconductive specimens collect charge when scanned by the electron beam, and especially in secondary electron imaging mode, this causes scanning faults and other image artifacts. For conventional imaging in the SEM, specimens must be electrically conductive, at least at the surface, and electrically grounded to prevent the accumulation of electrostatic charge. Conductive objects, such as metals, require little special preparation for SEM except for cleaning and conductively mounting to a specimen stub [31].

In our study, SEM was used to study the micro-morphology of the carbon blacks, as well as study the dispersion and morphology of carbon-cement samples (cf. § 2.4.1).

2.3.2 Resistivity Measurement

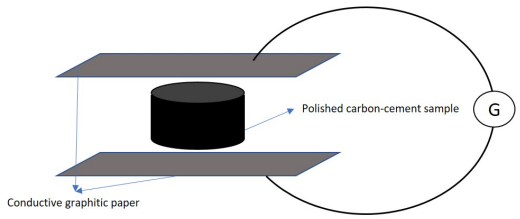

Figure 2.1: Resistivity measurement setup

The electrical resistance, R, of an object is a measure of its opposition to the flow of electric current. The electrical conductance, $G = 1/R$, and is the ease with which an electric current passes. The SI unit of electrical resistance is the Ohm (Ω), while electrical conductance is measured in Siemens (S) [32]. The resistance of an object depends in large part on the material it is made of: objects made of electrical insulators like rubber tend to have very high resistance and low conductance, while objects made of metals tend to have very low resistance and high conductance. However, resistance and conductance are not bulk properties, but extensive ones, meaning that they also depend on the size and shape of an object [32]. The resistance of an object is defined as the ratio of voltage across it (U) to current through it (I): $R = U/I$. This relationship is called Ohm's law, and materials which obey it are called ohmic materials. For a given material, the resistance is inversely proportional to the cross-sectional area and proportional to the length. The resistance of a conductor of uniform cross section, therefore, can be computed as $R = \rho\frac{l}{S}$, where l is the length of the conductor, measured in metres (m), S is the cross-sectional area of the conductor measured in square metres (m^2) and ρ is the electrical resistivity of the material, measured in Ohm-metres (Ω.m) [33].

Electrical resistance measurements were performed on a Solartron 1260-1287 device. The measurements consisted in applying a voltage ramp between the top and bottom sides of a carbon-cement electrode and registering the current passing through. Using Ohm's law, we could determine

the resistance of the sample and, after taking account of the sample geometry, deduce the resistivity. For each measurement the sample is squeezed between two graphitic papers and clamped to ensure a good contact. Electrodes linked to the measuring device are attached to each of the 2 graphitic papers and the measurement is carried out (Fig. 2.1). Two steps are defined: an open circuit phase, that lasts anywhere between 30 s and 1 min, to get rid of any residual sample polarization and a potentiodynamic phase, where a voltage from 0 to 10 V, is applied at a speed of 100 mV/s, while the time and the current are registered. These two consecutive steps are repeated two times for each sample, at a 30 second interval. This allows us to calculate error bars for the measurements.

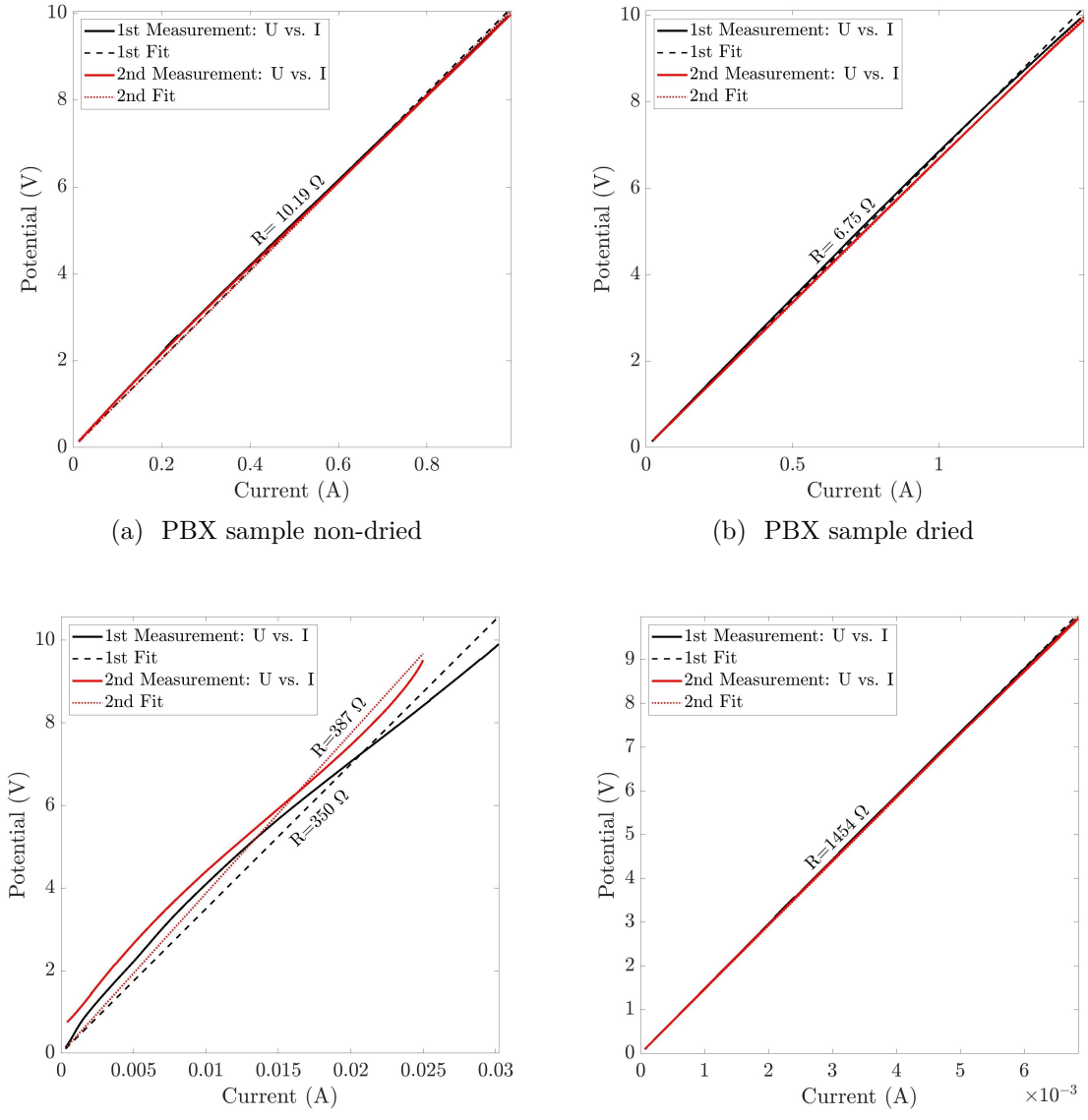

(a) PBX sample non-dried

(b) PBX sample dried

(c) AB sample non-dried

(d) AB sample dried

Figure 2.2: Example of resistance measurements of non-dried [(a) and (c)] and dried [(b) and (d)] states of two PBX and AB cement samples and their respective fits. PBX sample contains 9.64% carbon and a water to cement ratio of 0.8, while the AB sample contains 0.88% of carbon and a water to cement ration w/c = 0.42. Tests performed at an average sample age of 55 days.

As seen in Figure 2.2, we determine the resistance of the sample by fitting each of the two measurements and calculating the mean. We do this by assuming that our carbon-cement electrode is an ohmic component and then by fitting the curve with a line that passes through the origin: Ohm's Law. Of course, at higher voltages, when we dissipate more power, the temperature of the

samples can increase, which in turn may affect the resistance of the sample [34]: to avoid this we select the first part of the curve that manifests a more linear behaviour. Because the PBX sample is highly concentrated with carbon, the effect of drying is hardly seen, except for a small change in the value of the resistance. On the other hand, since the AB sample is less concentrated with carbon, we can see a clear effect: in Figure 2.2(c) the sample is still polarized after the first measurement, thus the curve of the second measurement is shifted and its resistance is higher. The presence of water solvates the ions, which enable ionic conductivity. After a first measurement the sample is polarized and manifests a slightly higher resistance to the current flow. In this case, we calculate a mean resistance and provide the corresponding error bars of the measurement. When the sample is dried, most of the water evaporates, thus no ionic conductivity and no polarization are seen in Figure 2.2(d): the resistance value is basically the same for the first and second measurements.

2.3.3 Capacitance Measurements

Measurements of capacitance are carried out using a method called cyclic voltammetry (CV), which is a type of potentiodynamic electrochemical measurement [35]. In a cyclic voltammetry experiment, the working electrode potential is ramped linearly versus time. After the set potential is reached, the working electrode's potential is ramped in the opposite direction to return to the initial potential. These cycles of ramps in potential may be repeated as many times as needed. The current (I) at the working electrode is plotted versus the applied voltage (E) to give the cyclic voltammogram trace [35]. The rate of voltage change over time during each of these phases is known as the experiment's scan rate v (V/s). The potential is measured between the working electrode and the reference electrode, while the current is measured between the working electrode and the counter electrode. The capacitance is proportional to the area under the curve I(E) and inversely proportional to the scan rate, following the relation:

$$C = \frac{\int_{E_1}^{E_2} I(E)dE}{2v\Delta E}$$

with $\Delta E = E_2 - E_1$ being the potential window of the measurement. By integrating between E_1 and E_2, we can determine the capacitance and thus deduce a specific capacitance (in mF/cm^2) for the samples [36].

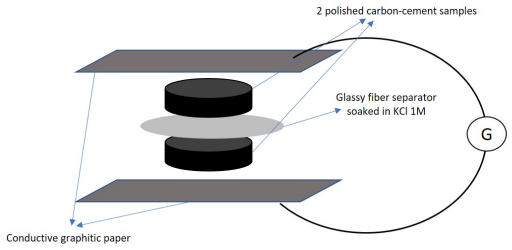

Figure 2.3: Capacitance measurement setup

Before the measurement, after being soaked in a potassium chloride solution for two-three hours, the two carbon-cement electrodes are taken out of the solution and placed on a paper towel in order to soak the excess of liquid on the surface. A sheet of glassy fiber filter paper, slightly bigger than the surface of the samples, is pre-cut and soaked in the 1M KCl solution used for the samples. The two samples sandwich the filter paper that electronically isolates the samples. The two samples are then sandwiched again between two sheets of graphitic papers, clamped, and after the electrodes are connected to both graphitic papers, the measurement is performed (Fig. 2.3). We run multiple cycles on the sample at different scan rates. Because the lower the scan rate, the longer it takes to perform one cycle, the number of cycles measured is different at different scan rates: larger for higher rates and smaller at lower rates. Typically, we measured 30 cycles at 500 mV/s, 15 at 200 mV/s, 10 at 100 mV/s, 5 at 50 mV/s and 3 at 20 mV/s. This allows a study on the dependence of the capacitance with the scan rate.

2.4 Carbon Black Nanoparticles

Carbon black is manufactured elemental carbon with customized particle size and aggregate morphology. Produced from the partial combustion or thermal decomposition of hydrocarbons, carbon black is primarily composed of elemental carbon (>98%). This number may vary based on its production process and final desired application, where carbon black may be doped with other elements like oxygen, nitrogen, or sulfur to impart solubility, better dispersion or binding properties to the material. The principal uses of carbon black are as a reinforcing agent in rubber compounds, especially tires, and as a black pigment in printing inks, surface coatings, paper, and plastics [37].

Carbon additives constitute one of the pillars of this study. Since its inception, multiple types of carbons have been incorporated into cement: activated carbon like Vortex or carbon blacks like Vulcan, Ketjen Black, different grades of PBX or Acetylene Black. These carbons come from different manufacturers and have different properties in terms of density, morphology, conductivity, surface area, water affinity or porosity. We studied the properties of these carbons in the lab and we describe them below. Since the core of my study was based around PBX55 (PBX) and Acetylene Black (AB), with some measurements done on Vortex and Vulcan, only these carbons will be described and compared in this section.

2.4.1 Scanning Electron Microscopy Measurements

Three levels of structural hierarchy exist in the carbon black system: they are composed of permanently fused "primary" particles or nodules, whose diameter is typically about 30 nm [38], to form aggregates of typical size 200-500 nm [Fig. 2.4(a)]. These aggregates display short range attractive interactions of typical strength 30 k_BT in oil [39] and form larger agglomerates of typical size (1-100 μm) through diffusion limited cluster aggregation [40]. Figure 2.4(a) displays the different scales of structural hierarchy and the fractal nature of the network present in carbon black. When dispersed in a liquid hydrocarbon, carbon black agglomerates form a space-spanning percolated network, even at small volume fractions (typically 1 to 5%) [41, 42, 43]. This fractal nature of the aggregates sets carbon black apart from other types of conductive additives such as carbon nanotubes, carbon fibers, graphene sheets, or graphite powder [44].

X-ray diffraction (XRD) is the experimental technique determining the atomic and molecular structure of a crystal, in which the crystalline structure causes a beam of incident X-rays to diffract into many specific directions. By measuring the angles and intensities of these diffracted beams, a three-dimensional picture of the density of electrons within the crystal is produced. From this electron density, the mean positions of the atoms in the crystal can be determined, as well as their chemical bonds or their crystallographic disorder [45]. In Figure 2.4(b), we examine the XRD pattern of several carbon powders found in literature [46]. The pattern of the graphite powder is characterized by a peak at $2\theta = 26.4°$, which is due to the ordered structure of graphite. For Vulcan and Ketjen Black powders, the XRD analysis shows an amorphous structure, whereas, for Acetylene Black powder, the XRD pattern indicates a more ordered structure compared to the other carbon blacks. Disordered structures for carbon blacks, in particular for Vulcan and Ketjen Black, are observed in Figure 2.4(c). A disordered lattice characterized by the absence of large-range order for the graphitical basal planes is typical of the amorphous carbons. Furthermore, all carbon blacks show a porous structure with a large presence of micro pores mainly in high surface area amorphous carbons [46].

To examine the morphology of our own carbons, we performed SEM imaging on some carbon samples. In order to observe the smallest possible units of our carbon agglomerates and avoid impurities, we dispersed a small amount (0.001 g) of each carbon sample in 20 mL flacons filled with acetone. Each flacon was manually agitated prior to the experiments and the suspensions were extracted with a pipette and placed on the sample holders. As our samples are electrically

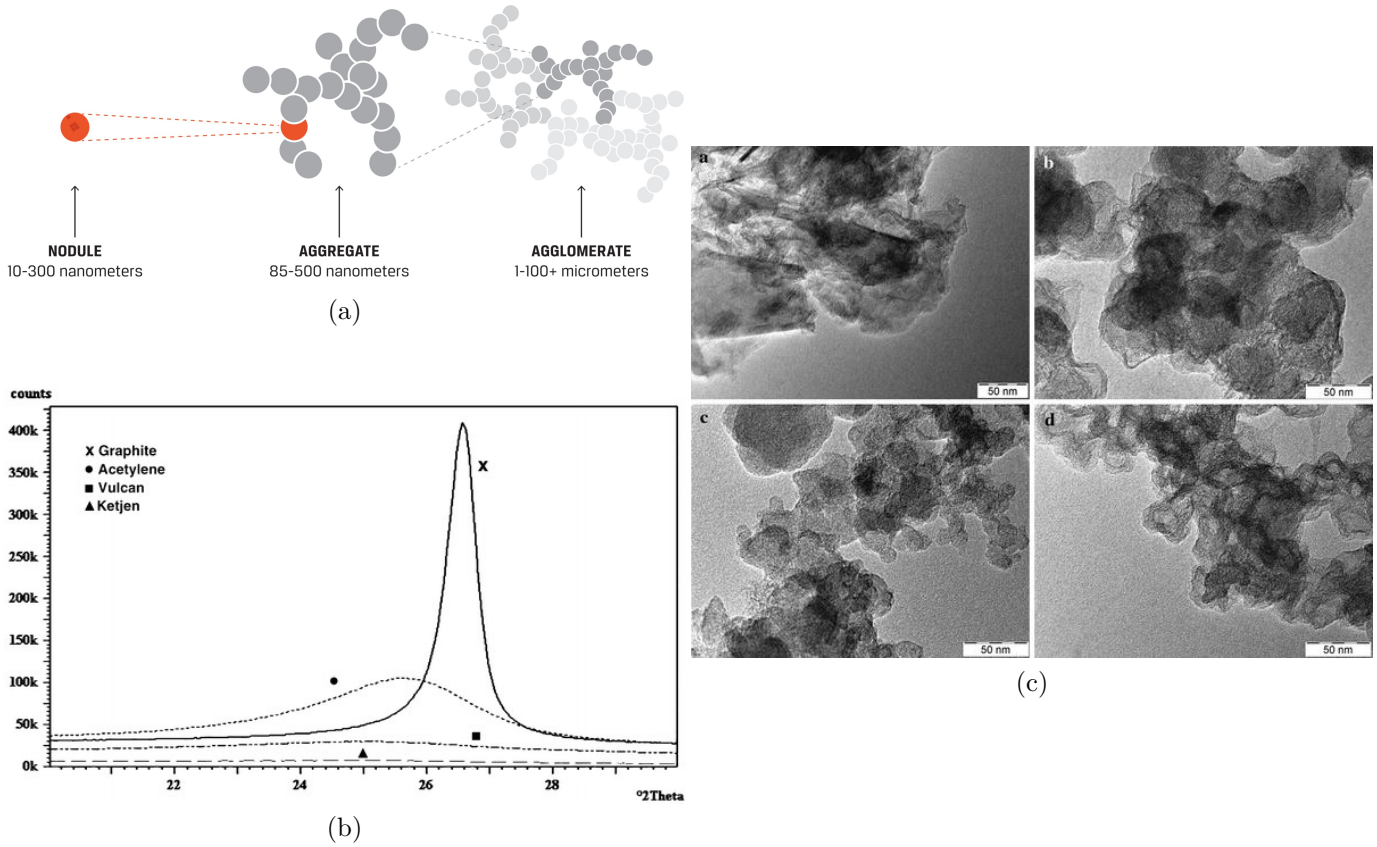

Figure 2.4: (a) Different scales present in the structural hierarchy of carbon black. Extracted from [40]. (b) XRD patterns from literature for graphite and several carbon blacks. Reproduced from [46]. (c) TEM images of different carbon blacks: a - Graphite, b - Acetylene Black, c - Vulcan XC-72R, d - Ketjen Black. Reproduced from [46].

conductive, the metal coating phase was skipped. The images were taken using a Zeiss Sigma 300 VP Field Emission Scanning Electron Microscope at varying accelerating voltages, as indicated in Figure 2.5.

We notice is that all four carbon types have different morphologies. Acetylene Black, at its smallest unit [Fig. 2.5(b)], seems to be made of sheet-like aggregates that combine in larger agglomerates [Fig. 2.5(a)] with sizes ranging from ten to a few hundred of micrometers. It seems to be very porous, which is consistent with our macroscopic observation, AB having the lowest density among the four studied carbons. PBX seems to be composed of flaky aggregates, but on our images [Fig. 2.5(d)] it looks more dense compared to AB. They combine into spheroids ranging in size from 10 to 50 μm. On Figure 2.5(c) it seems quite monodisperse, but these units may be able to combine in bigger agglomerates. In terms of morphology, Vulcan has very flaky base units, with nodules having around 10 nm in diameter [Fig. 2.5(f)], much smaller than PBX. They agglomerate into spheroids ranging from 5 to 15 μm. Vortex is the most unique among the four: it is made of sheets that range from 10 to 60 μm [Fig. 2.5(g)]. Although at its base unit Vortex is much bigger than the other 3 carbons, it does not seem to assemble into bigger agglomerates, which may be the reason that makes Vortex the easiest carbon to disperse in a solution. Since its smallest units are just sheets of carbon, Vortex is also the most highly dense among the other three carbons.

Although we did not perform more zoomed-in images, all four carbon types seem to have a disordered lattice, they seem to be lacking a long range order and all of them and Vortex seems to be having a highly porous microstructure. All four carbon types have different mesoscopic morphologies and they can affect the performance of our devices very differently. Since we are aiming at higher conductivities and higher porosities, performing electrical measurements gives us more insight into these properties.

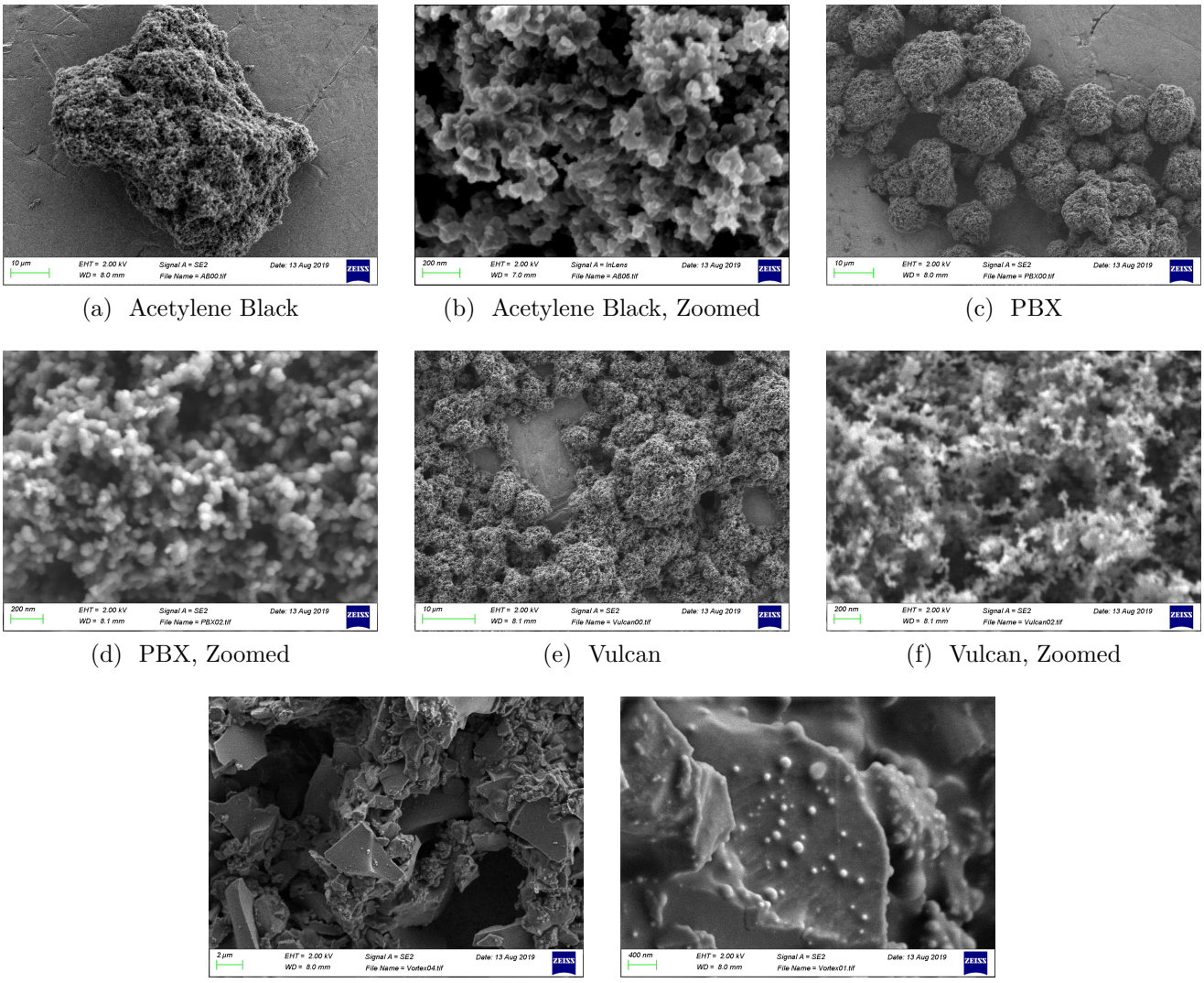

(a) Acetylene Black (b) Acetylene Black, Zoomed (c) PBX

(d) PBX, Zoomed (e) Vulcan (f) Vulcan, Zoomed

(g) Vortex (h) Vortex, Zoomed

Figure 2.5: SEM images of different types of carbon black performed at an accelerating voltage of 2kV. (a)-(b): Acetylene Black; (c)-(d): PBX; (e)-(f): Vulcan; (g)-(h): Vortex. Scale bar indicated in the image.

2.4.2 Resistivity

To test the resistivity of carbons we first had to turn them into pellets for an easy measurement. We have machined an instrument, consisting of three parts: two filled aluminium cylinders and one hollow. The desired amount of carbon was placed in between the filled cylinders and the whole would come together to squeeze the carbon to create a solid pellet, as represented in Figure 2.6(a). To apply the necessary pressure, we used a hydraulic press, which applied pressures in the range of 50 kN.

We measure the resistance of the carbon pellets according to the previously discussed protocol (cf. §2.3.2). Because the pellets were still very fragile, we kept them squeezed in between the two filled aluminium cylinders (whose resistance was measured separately: R=0.3 $\pm$ 0.02 Ω) and we applied the electrodes at their edges to measure the total resistance of the system. By considering our measuring setup, consisting of the carbon pellet and the two cylinders, as two resistors linked in series and by knowing the resistance of the cylinders, we deduce the resistance values of the carbon pellets: $R_{Pellet} = R_{Total} - R_{Cylinder}$, and consequently, their resistivities. It is worth noting that these measurements have been performed on a single sample for each type of carbon, thus the errors obtained do not include the errors of reproducibility. Pressing carbon into pellets can form small

denser regions in the sample, but also cavities, which can create variations into how the current is conducted. Measuring the resistances for a statistically significant number of samples for each type of carbon will give a more precise value for the resistivities of bulk carbon.

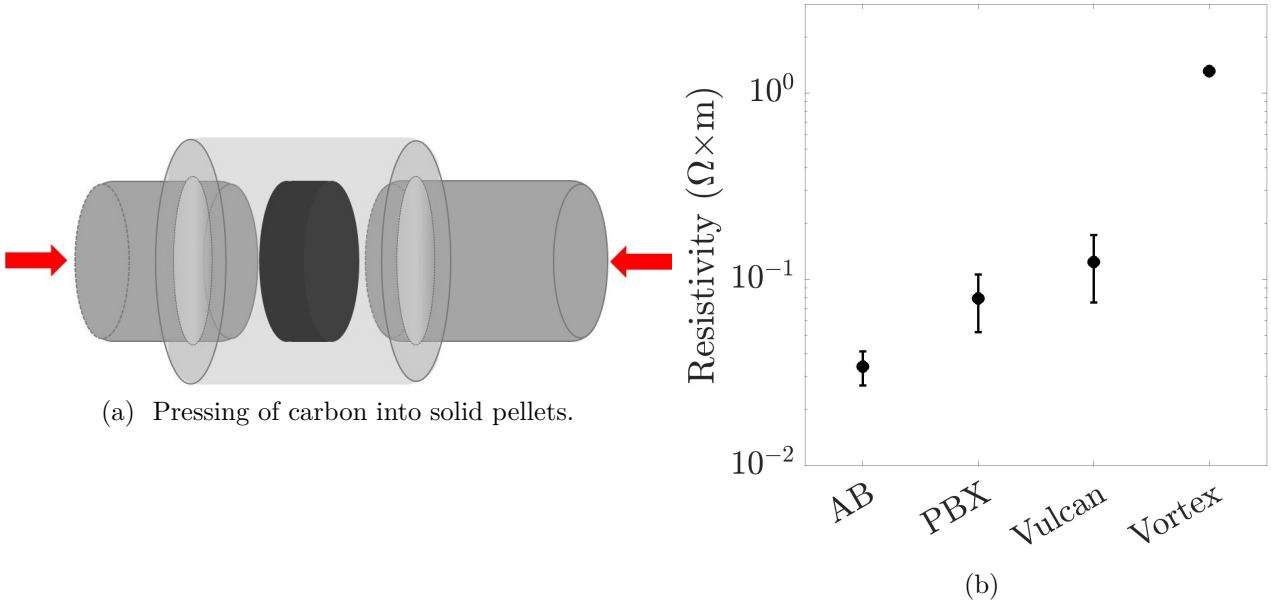

(a) Pressing of carbon into solid pellets.

(b)

Figure 2.6: Setup for resistivity measurements of carbon pellets. (a) The manufacture of pellets using machined parts and a hydraulic press. (b) Logarithmic comparison of the resistivity for the 4 studied carbon types.

We can observe in Figure 2.6(b) that Vortex's resistivity is about one order of magnitude higher than the resistivities of other carbons. This is not unexpected: Vortex is an activated carbon, which is known to contain lesser amounts of highly ordered graphitic carbon that conveys conductive properties. Nonetheless, its resistivity is low enough for it to be considered conductive and only further measurements on carbon-cement samples will prove if it can be a suitable candidate for supercapacitor devices. Vulcan and PBX are carbon blacks and are expected to contain a higher amount of graphitic carbon, hence their resistivities are both significantly lower than that of Vortex. Even though PBX is positioned lower than Vulcan, their resistivities are comparable. Their levels of dispersion and integration with cement will be the deciding factor in assessing their suitability for our device. Acetylene Black is produced through the combustion of acetylene gas and its manufacturing process conveys it a very high purity, as well as a high degree of graphitic carbon. We can observe this in Figure 2.6(b): AB is more than 2 times more conductive than PBX. In terms of conductivity, AB is an important candidate for capacity storage, but exploring how it integrates with cement will give us more insight into its potential usefulness. Overall, these results show us the limits of our systems and indicate to us the lowest resistivity values that can be expected for our samples.

2.5 Errors and homogeneity

Cement is a highly heterogeneous material, having multiple compounds participating at the chemical reaction, as well as different phases (alite, belite, celite, etc.) and impurities (titanium dioxide, magnesium oxide, carbon dioxide, potassium oxide, etc.). Two casts of cement are never chemically the same [47, 48]. Variances can be caused by material weighting, use of different batches, material transferring, poor dispersions and segregation of carbon during casting. All this factors can weight in and induce errors when comparing two samples. On top of that, there are other sample preparation and measurement errors that could have a noticeable effect: since the contact with the electrode is depended on the parallelism of the sample surfaces, errors can occur during the cutting

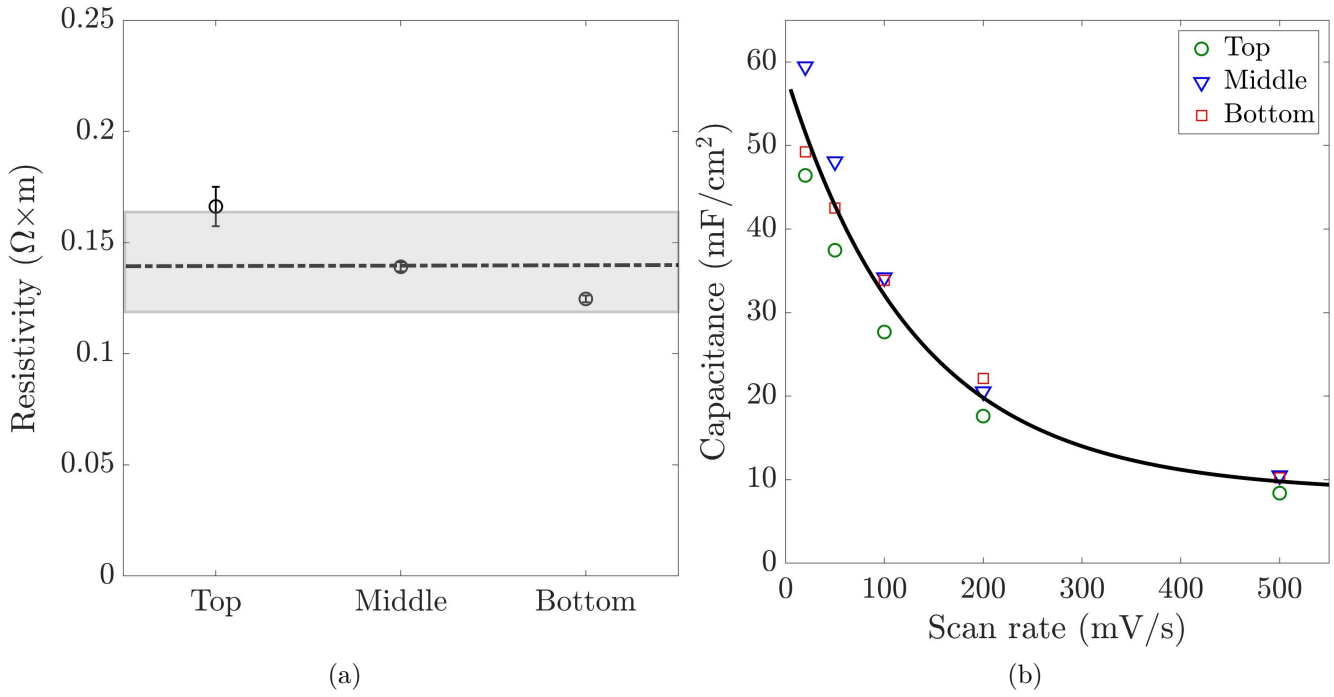

Figure 2.8: (a) Resistivity values for samples corresponding to 3 positions in the same PBX 11% cylinder. R = 0.143 ± 0.023 Ω.m, a dispersion of 16%. (b) Capacitance values and average at different scan rates for top, middle and bottom samples coming from one cylinder of PBX at 11%. Tests performed at a sample age of 100 days.

process; the polishing process is crucial since it determines the surface roughness (important for good contact), as well as the thickness of the samples. It is imperative to have a good grasp of these factors in order to correctly assess the precision of our measurements and the limits of our system.

2.5.1 Within the same sample

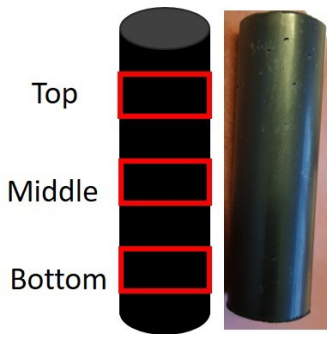

Figure 2.7: Top, middle and bottom: three positions studied inside one carbon-cement batch (cylinder).

One of the first questions that can arise is: how homogeneous are the carbon-cement cylinders that we make and is there any carbon segregation during casting? We have studied the homogeneity of a cylinder containing 11% wt of PBX. We measured the resistivity and capacitance of samples taken at 3 locations within the same cylinder: top, middle and bottom (Figure 2.7).

In Figure 2.8(a) we observe the resistivity corresponding to the 3 positions within the cylinder, having an average of 0.143 ± 0.023 Ω.m, which corresponds to a dispersion of 16%. We see a decreasing trend that goes from top to bottom. This is a peculiar result: in the case where the position of the sample mattered, we expected a segregation effect where the heavy cement and water would move to the bottom and the lightweight carbon would move to the top. Thus, the concentration of carbon at the top would increase and create a region of increased conductivity. We observe the opposite trend: the resistivity seems to decrease from top to bottom. We can expect another mechanism to be involved or the result does not represent an actual trend. We will compare with capacitance values in order in order to shed some light on it.

In Figure 2.8(b), we can see capacitance measurements results at different scan rates cor-

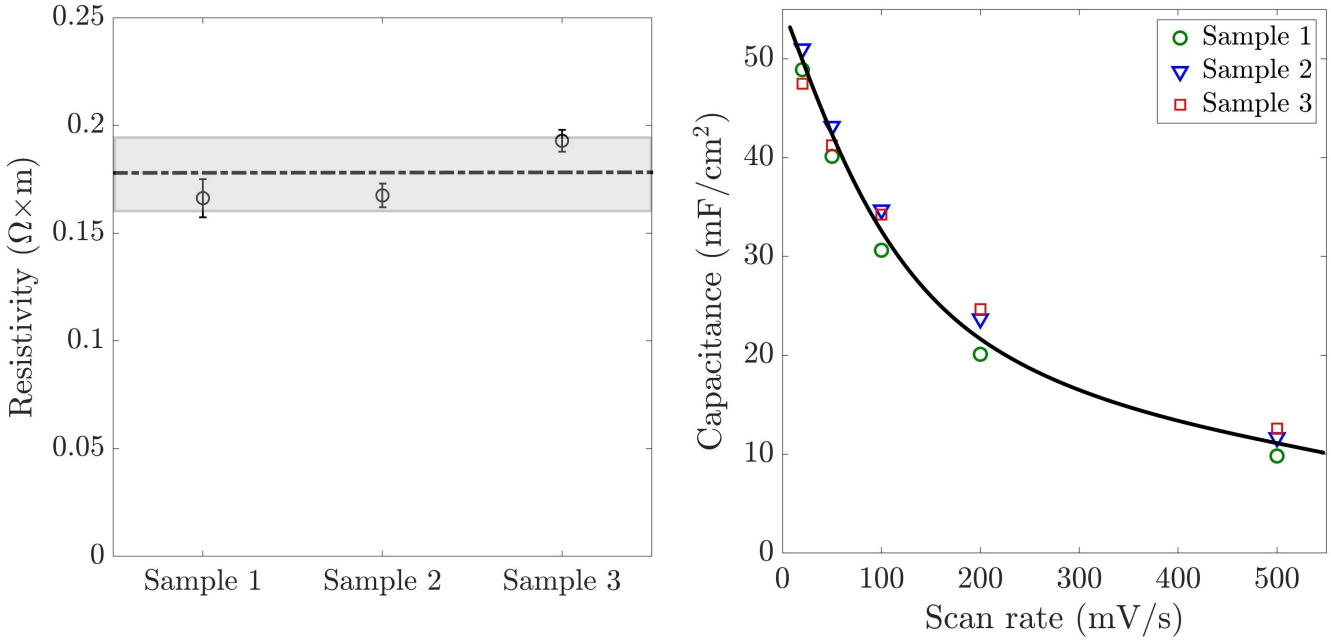

Figure 2.9: (a) Resistivity for top samples extracted from 3 different batches of PBX (11% wt). Error bars represent the error associated with each measurement. (b) Capacitance values and average at different scan rates for samples extracted from 3 different batches of PBX (11% wt). Tests performed at a sample age of 100 days.

responding to the 3 positions within the same sample. We observe that throughout most of the scan rates, the middle sample has similar values to the bottom one. However, it has much higher values than both the top and bottom ones at lower scan rates. This discontinuity in the capacitance performance tells us that there is not an increasing, nor decreasing trend from top to bottom, as suggested by the previous resistivity result. We can suspect that the capacitance is not sensitive to small changes in resistivity. Moreover, it seems that capacitance values seem to be more sensible to change at lower scan rates, where at lower speeds processes like particle diffusion become more impactful. Although the value of the error is proportional to the value of the capacitance at different scan rates, it remains consistently at 12-15%.

2.5.2 Different batches

To what extent can we consider our sample preparation repeatable, or what is the error linked to the synthesis of the samples? We compare three batches made with the same chemical composition (cement, water and carbon). We performed resistivity and capacitance measurements on these three samples containing 8.4 g of PBX carbon, the percentage of carbon used being 11% wt. For each of the three batches we compared samples from the upper part of the cylinders, which were cut and polished to the appropriate size and roughness.

On Figure 2.9(a) we can observe the resistivity measurement results of the samples from the three batches. We see that our samples perform very similarly: we obtain an average of 0.175 ± 0.017 Ω.m, or a dispersion of about 9% that we can expect at each synthesis. We performed cyclic voltammetry experiments on samples taken from the top part of the same three batches (same region as the samples taken for resistivity measurements). On Figure 2.9(b) we can observe the capacitance values for each sample at various scan rates, as well as the average. The dispersion we have to expect from our measurements is between 9.8% and 3.8% depending on the scan rates. Overall

these 2 results give us an important understanding of how slight variations in mixing, dispersion or casting can influence the electrical properties of our composite material. They allow us to claim that our samples are very similar, highly reproducible and that the dispersion of the results due to the synthesis is about 10%.

2.6 Ensuring a good sample/electrode contact

Ensuring a proper contact between our carbon-cement electrodes and the measuring electrodes is a crucial element in obtaining repeatable results. It required a more rigorous polishing of the electrodes. We also attempted to make our electrode surfaces as plane and smooth as possible, in order to obtain a the better inter electrode contact. On top of that, we used flexible graphitic paper as links between our electrodes and the measuring electrodes to secure a better contact.

2.6.1 Discussion on measuring setups

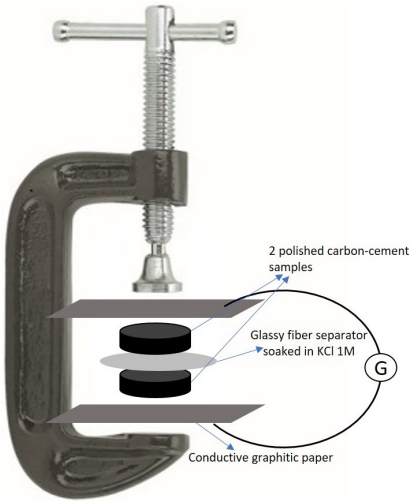

Figure 2.10: Applying pressure on the samples with a C-clamp.

The first setup used in our capacitance measurements included an industrial C-clamp to ensure a good contact. The 2 polished carbon-cement samples would sandwich a KCl soaked glassy fiber paper and the clamp would be used to keep it all together (Fig. 2.10). Involving a C-clamp created several problems: achieving a proper force distribution was complicated and the balance between a loose sample and breaking the sample was very difficult. We realized that by applying different pressures on our samples we were creating different experimental conditions for them by varying the contact. Controlling the pressure applied to the became a priority.

We attempted using a new setup [Figure 2.11(b)], where we ensure a better distribution of the force over the entire sample. The sandwiched electrode would be placed in between two metal cells and the whole would be clamped using an industrial C-clamp. By first transmitting all the force to the cell, we achieved a better force distribution, which translated in fewer broken samples. However, we still could not properly control the forces that we were applying, because the setup was rigid and our samples varied in thickness. On the other hand, a clamp is a very powerful tool, being able to apply several kN of force per revolution, depending on its size. Thus a clamp is not the ideal instrument for an accurate measurement.

Finally, we designed homemade measuring setup. We used a spring to control the force applied. An important property of a spring is its constant, which describes a linear relationship between the force applied on the spring and the deformation it exhibits. Thus, by knowing a spring's constant and by measuring its deformation, we can easily determine the force it is sustaining. In the setup [Figure 2.11(c)] we kept the principle of the cell, but in our case the upper part is a moving cylinder connected to a spring. When the sample is in place and the necessary screws are tightened, we use a wrench to slowly lower the nuts and deform the spring by the desired amount, thus applying a precise amount of force at each experiment. The spring we chose for our experiments has a constant $k = 40.15$ N/mm and allows us to apply on our samples a force in the range of 0 and 2600 N.

We used the pressure cell to measure the evolution of the resistivity and the capacitance for different applied pressures. We chose again a carbon-cement sample containing 11% wt PBX, whose results are reported in Figure 2.12. We notice in Figure 2.12(a) how crucial the application

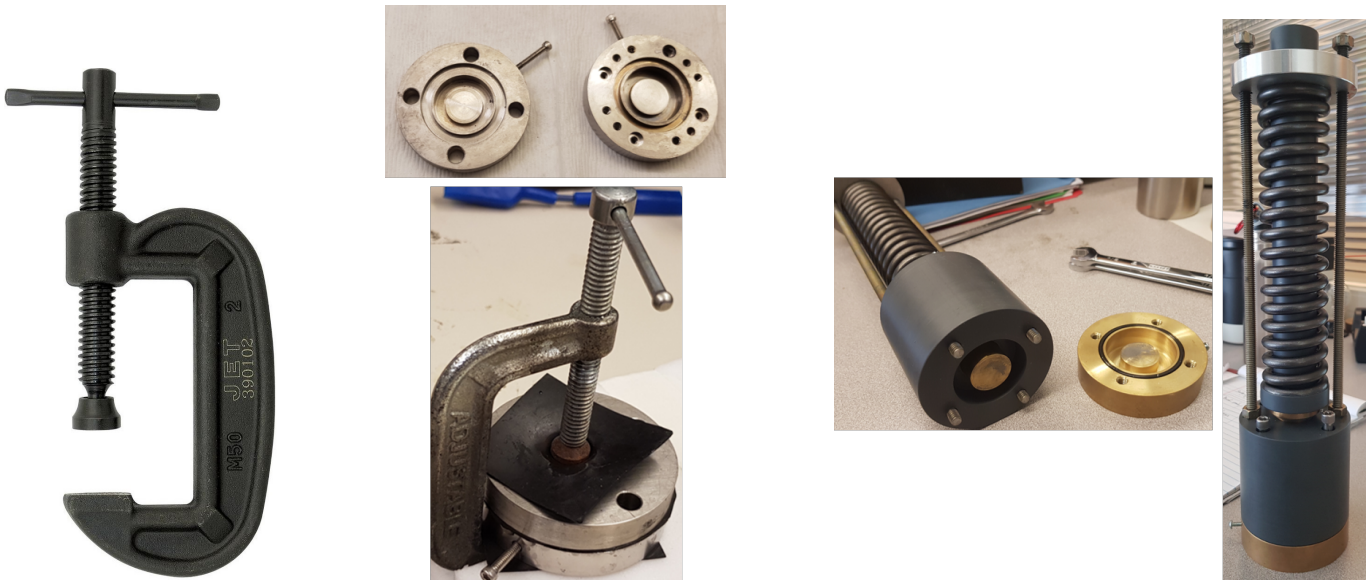

(a) (b) (c)

Figure 2.11: Measuring setups: (a) C-clamp. (b) Clamp and cell. (c) Pressure cell used for experiments reported in this document.

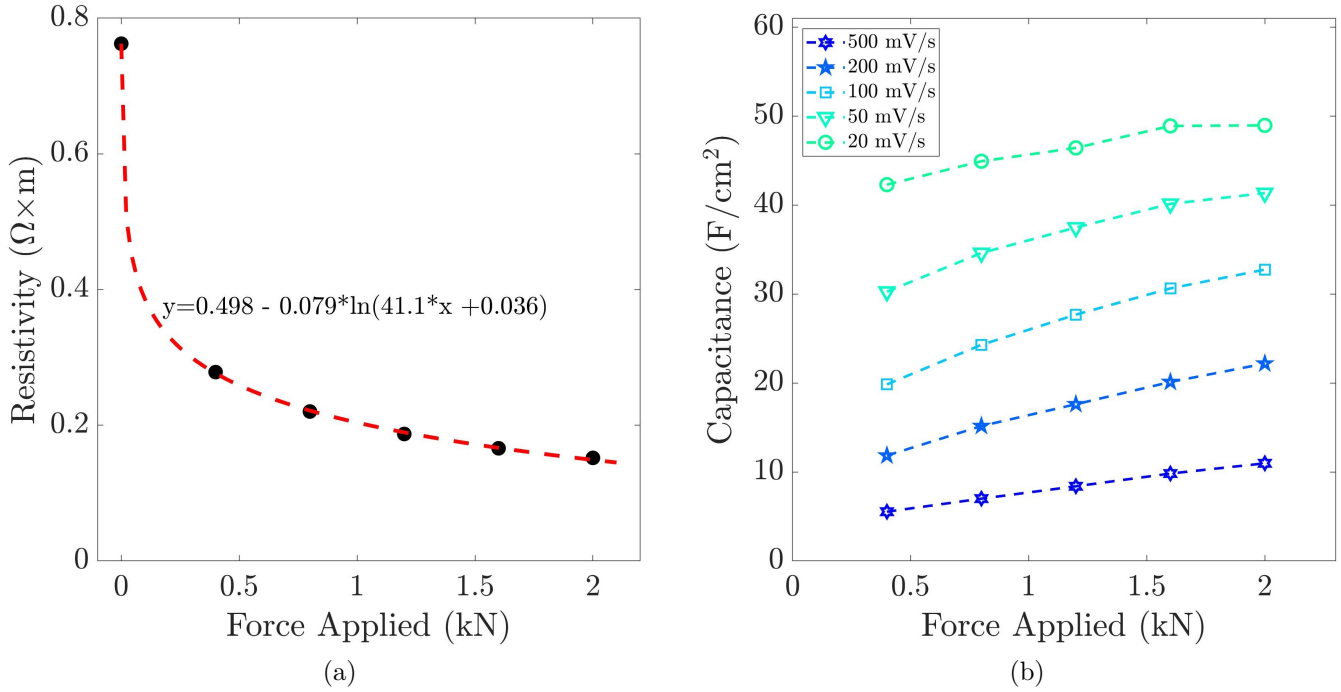

(a) (b)

Figure 2.12: (a) Resistivity as a function of the applied force. The first point corresponds to no force applied on the sample, excluding the weight of the spring. The second point corresponds to a force of 400 N and it continues with increments of 400 N. (b) Capacitance measurements for different scan rates as a function of the applied force. tests performed at an average sample age of 100 days.

of pressure on our samples is: there is more than a 4 fold decrease in resistivity between 0 N and 2000 N. For increasing pressure, we notice a steady decrease in the resistivity: we go from 0.28 Ω.m to 0.15 Ω.m, i.e. a decrease of more than 45%. We can notice that the decrease in resistivity (or the increase in conductivity) is logarithmic. A conclusive explanation of this phenomenon has not been found in literature. The forces we apply are too weak to cause a change in the packing factor or any

other structural changes in the cement, that require pressures in the order of tens of MPa [49]. Thus we can conclude that the effect can only be due to the improvement in the contact of the electrode. It seems intuitive that the resistivity can only drop to a certain value, since there is a limit to how "close" the surfaces of the electrodes can get. However, it is likely that this limit has not yet been achieved and that measuring it at higher applied forces would compile a more accurate fit. Increasing the pressure, on the other hand, can lead to a deterioration or destruction of the sample, which can also set an independent limit on the obtainable resistivity. It is possible that at the beginning, before the pressure is applied, there are many local points on the surface of the electrode that can benefit from an improved contact, but as more pressure is applied and the space for change decreases, so does the effect brought by the increasing pressure.

In Figure 2.12(b), for each scan rate we can observe an increase in capacitance for increasing applied force. Overall, it seems to be linear for all scan rates, however, compared to the resistivity measurement, we do not have a measurement at 0 N force applied for the capacitance as a reference. Thus, it is also possible that what we are visualizing is the reaching of the plateau part of an exponential, which means that we can apply the same speculation points we used for resistivity here as well. This difference between the sample at 400 N and 2000 N can vary from 25% at low scan rates to 50% at high scan rates. It seems like the samples at lower scan rates are less affected by the change of external conditions, a phenomenon that we observe through many of our samples. We will speculate on the reasons that may cause this in §3.

Overall, what we need to deduce from these two results is that the pressure applied on the samples is a very important parameter that has to be controlled in all experiments. The values we obtained here exceed by far the errors associated with the position of the sample in the cylinder or the chemical synthesis, thus the result is significant and machining the pressure cell was totally justified. In the rest of the report we chose a fixed force that we applied to all our samples in our experiments. Since deforming the spring to 2000 N is time consuming and requires more physical effort, we chose the value 1200 N to be our reference.

Chapter 3

Results and Discussion

Our study was one of exploration and optimization, with the goal of finding the best candidate for a supercapacitor energy storage device. To achieve this goal, we studied more than a hundred samples, synthesized with 4 different carbon types and varying parameters (such as water to cement ratio, different carbon concentrations, etc.) and performed tests of resistivity and capacitance. We defined several essential parameters that can have a direct impact on the electrical measurements:

1. Carbon type
2. Carbon concentration
3. Water to cement ratio
4. Additives

Each of these parameters will be detailed and explained in the sections bellow.

3.1 Carbon Type

Each carbon type has intrinsic properties, thus each sample made with a different type of carbon displays different properties from the others. To study the influence of the type of carbon, we synthesized one cylinder for each of the four types of carbon at the maximum (experimentally accessible) concentration and performed resistivity and capacitance measurements on them.

As seen in Figure 3.1(a), Acetylene Black and PBX samples have the lowest resistivities out of the four types of carbon, approaching to their respective bulk values. This result is important for two reasons: it suggests that the chemical structure of both these carbons is not altered/does not interact with the cement compounds, since the electrical properties do not seem to be affected; we speculate that the morphology of the particles allows them to be easily dispersed in order to form a highly percolated carbon network in the cement matrix. AB and PBX are the long-term candidates for our energy storage device. Compared to them, the sample prepared with Vulcan has a much higher resistivity, one order of magnitude higher than Vulcan alone. Vulcan particles might be affected by the rich chemistry unfolding in cement during the casting period, or it is not properly dispersed. It is also possible that there could still be an important improvement for Vulcan samples if we could disperse more carbon in them. The most surprising result comes from Vortex: while being a fairly good conductor as bulk carbon, at 1.3 Ω.m, the carbon-cement mix is a insulator at more than 6000 Ω.m. As we know little about the exact chemical composition of Vortex, it is hard to come to any conclusive explanation. The most likely explanation is that Vortex interacts with compounds in cement and its conductive properties are reduced. A more detailed study into Vortex is required to point out an exact cause of this phenomena. In Figure 3.1(b) we see the results of capacitance measurements performed on the same samples at a scan rate of 100 mV/s. As expected

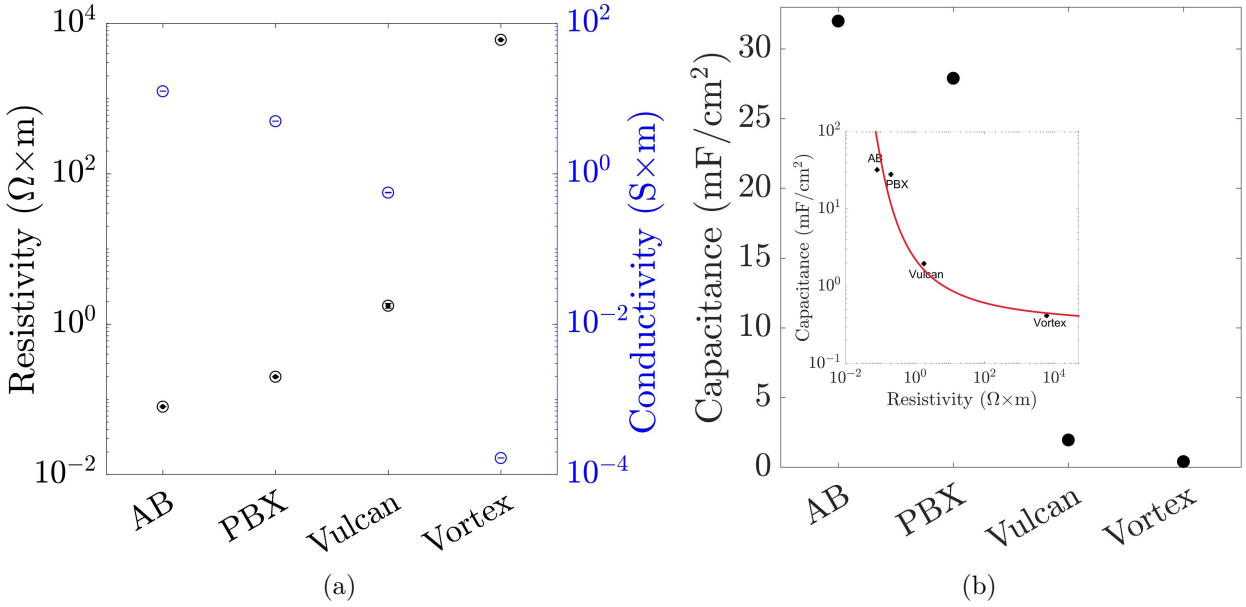

Figure 3.1: Comparison of resistivity (a) and capacitance (b) for cement samples with the 4 types of carbon at maximum concentration out of total weight and w/c of 0.8. AB - 8.2% wt, PBX - 11.1% wt, Vulcan - 9.8% wt and Vortex - 24.5% wt. Resistivity measured for dried samples. Capacitance values presented at a scan rate of 100 mV/s. Inset capacitance vs. resistivity presented in a log-log scale. Tests performed at an average sample age of 40 days.

from resistivity results, Acetylene Black and PBX have the highest capacitance value at this scan rate, at 32 and 29 mF/cm^2, while Vulcan's and Vortex's capacitances are very low, close to zero. This suggests a link between capacitance and resistivity. In a supercapacitor, the charge is accumulated inside the capacitor via ionic transport and intercalation of ions into the active material structure, therefore higher electronic conductivity of the material structure is needed for higher capacitance. The situation is slightly more ambiguous for Vulcan: while not as conductive as AB or PBX, its capacitance is closer to that of Vortex at 1.97 mF/cm^2. There must be other mechanisms involved besides the resistivity that would explain such an important difference.

In Figure 3.2 we can see the cyclic voltammetry (CV) curves of cement samples with the four studied carbons performed at a scan rate of 100 mV/s. Vortex and Vulcan samples' CV curves can be viewed as lines: the current output is directly proportional to the applied potential, which suggests very little or no energy storage. The cement sample containing AB has a more curved shape and spans over a region of more than 60 mA, which gives it a high potential for energy storage. The cement sample prepared with PBX, on the other hand, spans over a smaller region of about 35 mA, but has a different shape that strives towards a rectangle. An ideal supercapacitor is a device that stores high amounts of energy and is capable of releasing or absorbing it very quickly, thus it is characterized by regions of fast charge and discharge [50]. Because a rectangle is the shape of the CV curve of an ideal supercapacitor, the PBX sample is the one that approaches the most to our idealized model. We can see that PBX has a very fast charge between 0 and 0.25 V, then a fast discharge between 1 and 0.75 V, both followed by regions of steady charge/discharge, that are almost constant. Even though both AB and PBX have high capacitance values, PBX has more promise in terms of efficient energy storage.

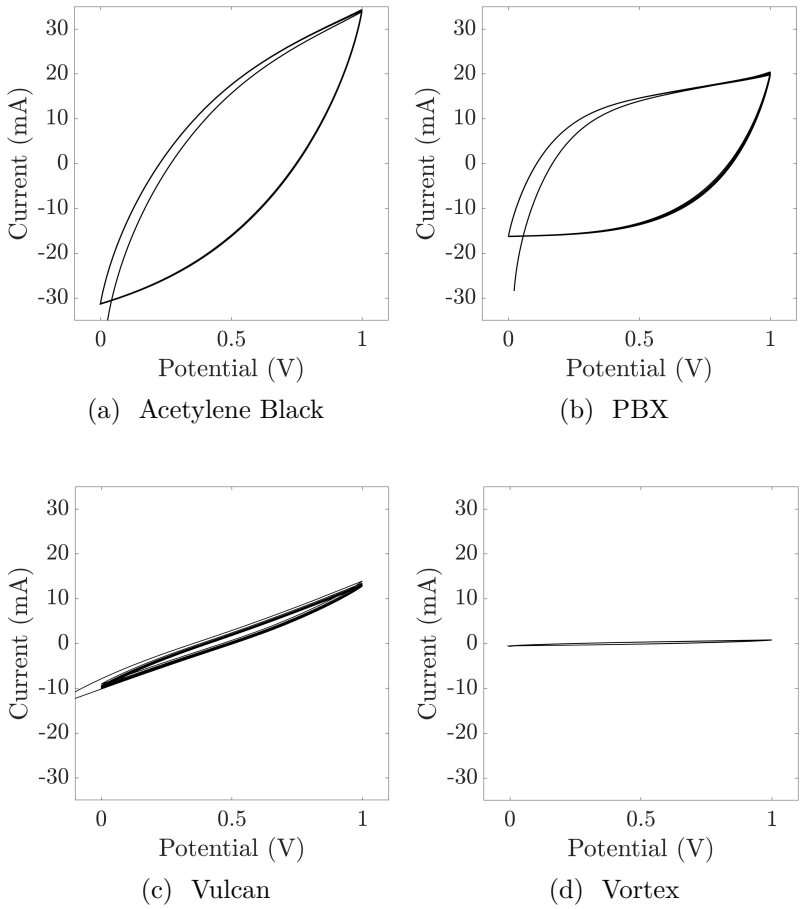

(a) Acetylene Black (b) PBX

(c) Vulcan (d) Vortex

Figure 3.2: Voltammetry curves, performed at 100 mV/s, 50 cycles, corresponding to cement samples with the four types of carbon nanoparticles at maximum concentration out of total weight: AB - 8.2%, PBX - 11.1%, Vulcan - 9.8% and Vortex - 24.5%. Tests performed at an average sample age of 40 days.

3.2 Carbon Concentration

To study the influence of carbon concentration upon the performance of carbon-cement composites we synthesized two batches of PBX and AB samples at different carbon concentrations and compared how these samples' resistivity and capacitance output scaled with the carbon content. Both batches were made at the same water to cement ratio w/c = 0.6: for AB we synthesized samples at 0%, 1.11%, 2.20%, 3.26%, 4.31%, 5.33% and 6.32%, percentage of total weight; for PBX we synthesized samples at 0%, 1.48%, 2.91%, 4.31%, 5.66%, 6.98% and 8.26%.

In Figure 3.3 we report the resistivity for the two series of samples prepared with AB and PBX. Resistivity values are highly impacted by the dryness of the samples. On condition that a percolated carbon network is established, in dried samples the dominant conductivity is the electronic conductivity due to the network of carbon particles, while in non-dried samples there are present two (mostly) independent conductivities: electronic and ionic, due to the ions present in cement [51]. We introduce the percolation threshold: it is the lowest concentration of filler at which an insulating material is converted to a conductive material. This means that percolation threshold is the lowest concentration of filler at which an electrical pathway is formed throughout a sample [52]. A good reference point for us is the comparison of the dried and non-dried conductivities. By comparing these two states we can point out the percolation points for each series. Thus, the percolation threshold is reached when the values of the non-dried and dried samples coincide at the same carbon concentration. We notice that for cement samples prepared with AB, it occurs around

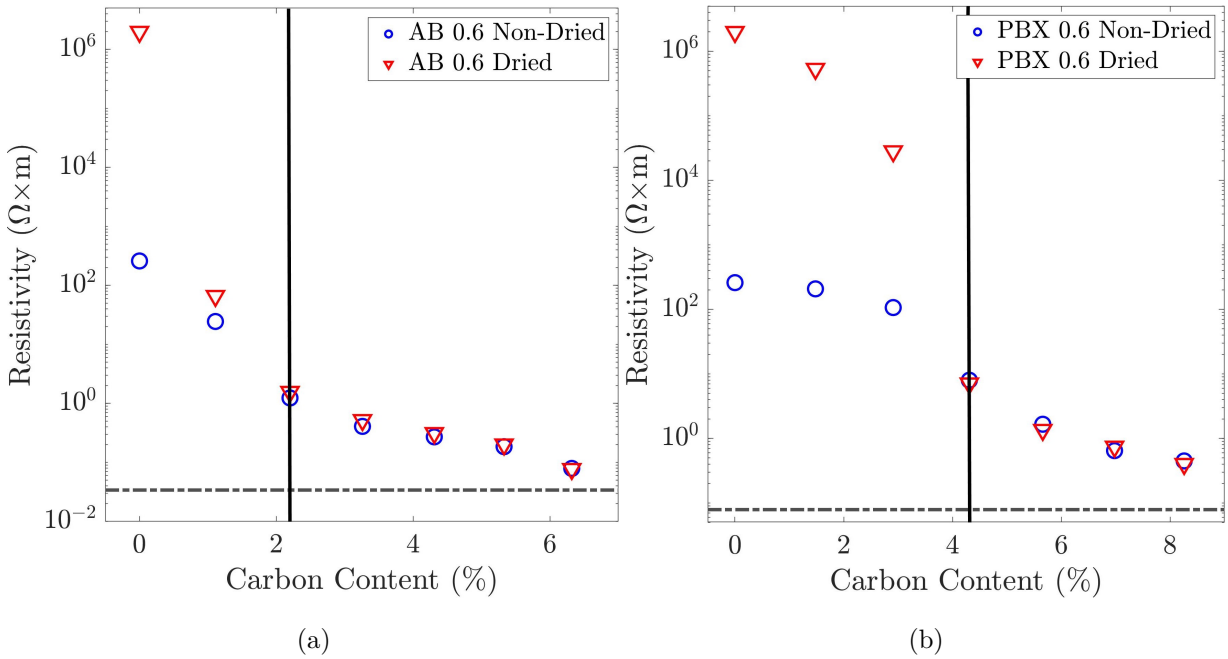

(a) (b)

Figure 3.3: Resistivity values vs. carbon content for two series of samples prepared with Acetylene Black (a) and PBX (b) synthesized at w/c = 0.6. Samples measured in dried and non-dried states. Dashed bottom lines correspond to the resistivities of the respective pure carbon. Tests performed at an average sample age of 55 days.

1.7%, while for cement samples made with PBX it is around 3.6%. Cement samples with AB are more conductive, as well as less dense than those made with PBX, so this percolation shift towards lower concentrations, compared to those made with PBX, is not surprising for the ones prepared with AB. The second thing we can take out of these graphs (Figure 3.3) is that the resistivity scales with the carbon content: by adding more carbon we continue to decrease the resistivity. This resistivity would continue to decrease until it reaches a constant value, very close or equal to the value of the bulk carbon [53]. When taking into account the error bars of our measurements due to the synthesis, we see that we are very close to reaching the pure carbon value for AB, whereas there is still room for improvement for PBX.

In Figure 3.4 we see the capacitance values at different scan rates for the same two series of cement composites prepared with PBX and AB. The capacitance values also scale with the carbon concentration for each scan rate. This is in agreement with the increasing conductivity observed in Figure 3.3, but can also be due to the increased quantity of carbon, which in turn adds more porosity for ionic storage [54]. An interesting thing to point out is that the the points where the capacitance starts increasing drastically coincide with the "resistivity percolation points": capacitance values take off only after reaching the electronic percolation concentration in both series. This once more strengthens the link between conductivity and capacitance in supercapacitors. We can see it as well in Figure 3.5: there is an obvious decrease in capacitance when the resistivity is increasing. This decrease seems to be more linear on a log-log scale for AB, which suggests a power law decrease. However, this "line" is more difficult to visualize for PBX and it may be due to a different mechanism of dependency for different carbon types. Overall, this figure shows that capacitance does scale with the resistivity and that there is a range of values for resistivity that has to be reached in order to achieve high capacitance (at least for PBX and AB).

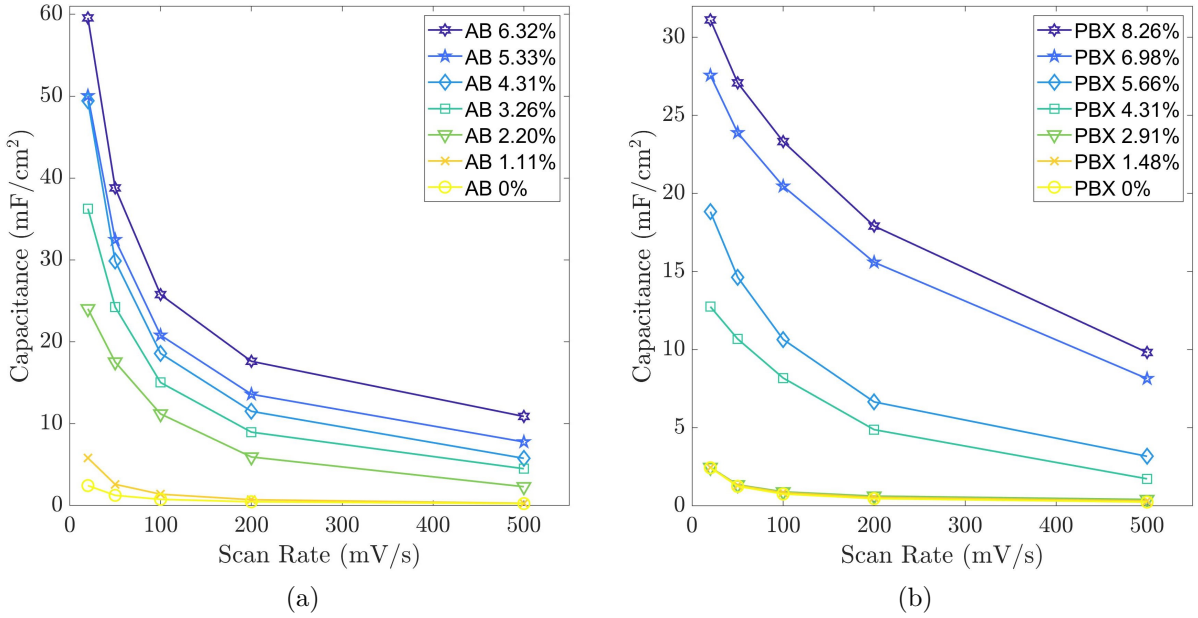

Figure 3.4: Capacitance vs. scan rates for two series of samples prepared with Acetylene Black (a) and PBX (b) synthesized at a w/c = 0.6. Tests performed at an average sample age of 60 days.

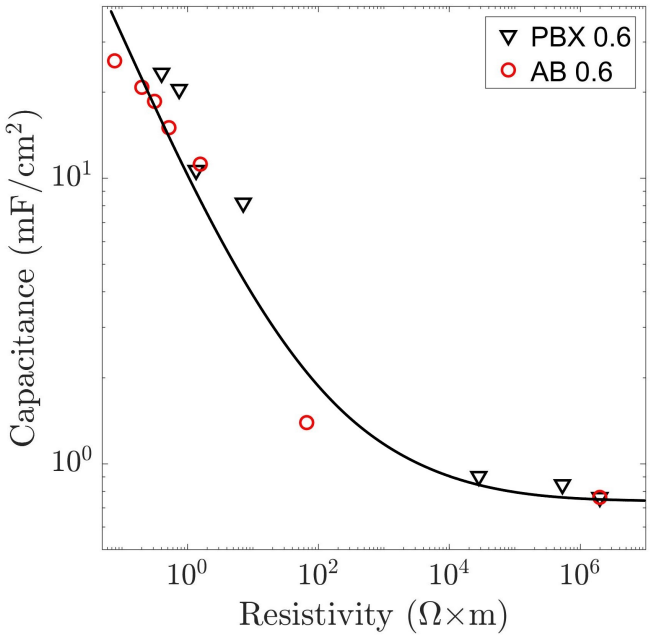

Figure 3.5: Evolution of capacitance with resistivity for cement samples prepared with PBX and AB carbons at a w/c = 0.6. Decreasing concentration of carbon from top to bottom and from left to right. Capacitance values measured at 100 mV/s. Resistivity values determined on dried samples.

3.3 Water to Cement ratio (w/c)

To study the influence that the water to cement ratio has upon the performance of our samples, we synthesized multiple batches of PBX and AB samples at different carbon concentrations and w/c and compared how these samples' resistivity and capacitance values varied under different parameters. In Figure 3.6 we compare resistivity values for series of AB and PBX synthesized at 3

different w/c values: 0.42, 0.6 and 0.8. Just as in Figure 3.3, we see that the scaling with carbon concentration is consistent at different w/c both for PBX and AB. The first thing to notice is that the minimum achieved resistivity is lower at increasing w/c, which is consistent with the addition of more carbon. We can notice is that the electronic percolation points are shifting at different w/c, as seen in Figure 3.7. For both samples containing PBX and AB, when the water to cement ratio is increasing, the electronic percolation points are shifting towards higher concentrations. This change seems to be linear and could allow us to predict the percolation points in this range of w/c. For PBX we have: $P_t = 8.67R_{wc} - 1.14$ and for AB: $P_t = 0.92R_{wc} + 1.26$, where P_t is the percolation threshold and R_{wc} is the water to cement ration. Cement porosity is highly controlled by the amount of water introduced in the mix [55]. When casting, the water that is not consumed by the hydration reaction may leave the concrete as it hardens, resulting in microscopic pores [56]. Thus increasing the w/c means increasing the porosity of the matrix. This effect might be responsible for the shift in percolation points: a higher porosity means more carbon is required to fill the pores, thus more carbon is needed to create a percolated network.

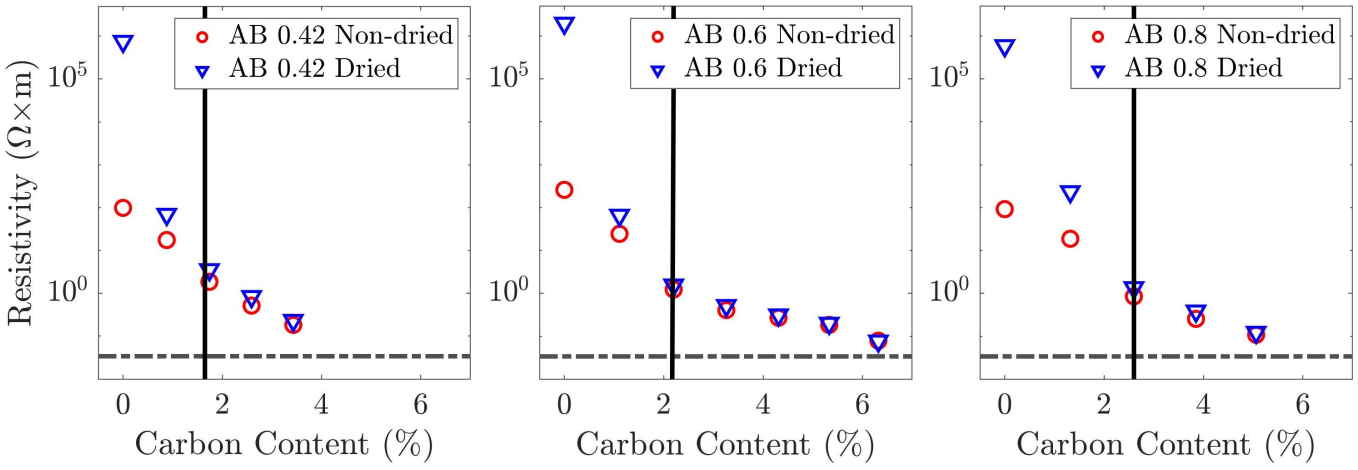

(a) Acetylene Black

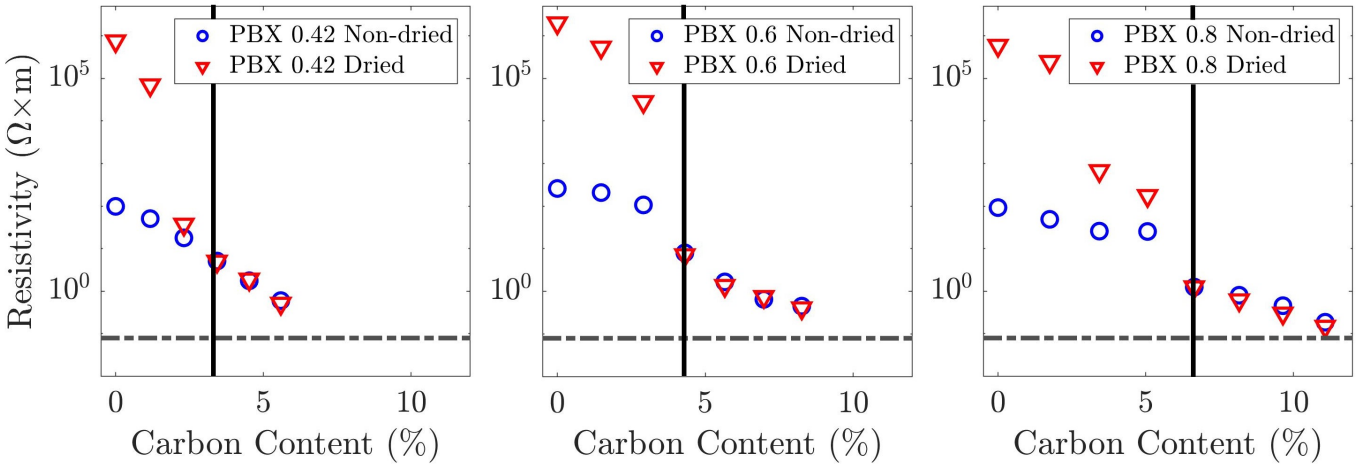

(b) PBX

Figure 3.6: Resistivity values for for three Acetylene Black and three PBX series at three different water to cement ratios: w/c = 0.42, 0.6 and 0.8. Each sample has been measured two times in a dried and non-dried state: for each graph, each two measurements in a dried and non-dried state correspond to the same sample. Dashed bottom lines correspond to the resistivities of the respective pure carbon. Tests performed at an average sample age of 55 days.

In Figure 3.8 we compare capacitance values for two PBX carbon-cement composites at w/c = 0.42 and 0.6. As with the resistivity values, the capacitance values are consistent with the

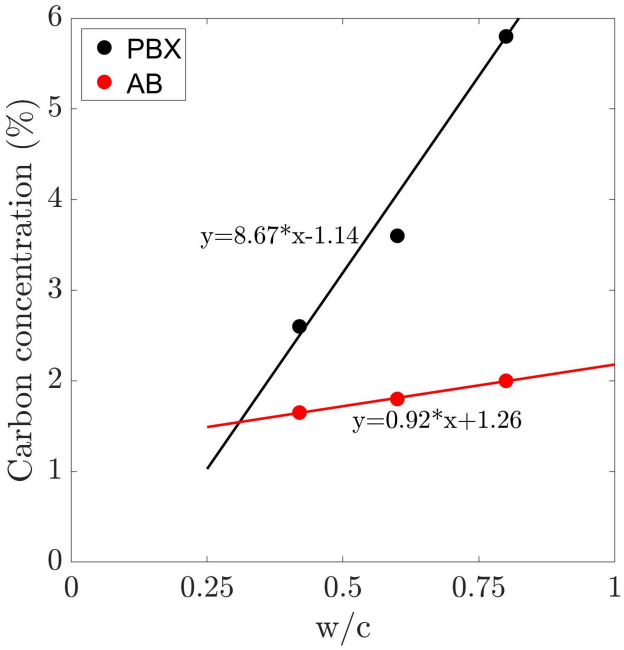

Figure 3.7: Evolution of the carbon percolation threshold with the w/c for PBX and AB.

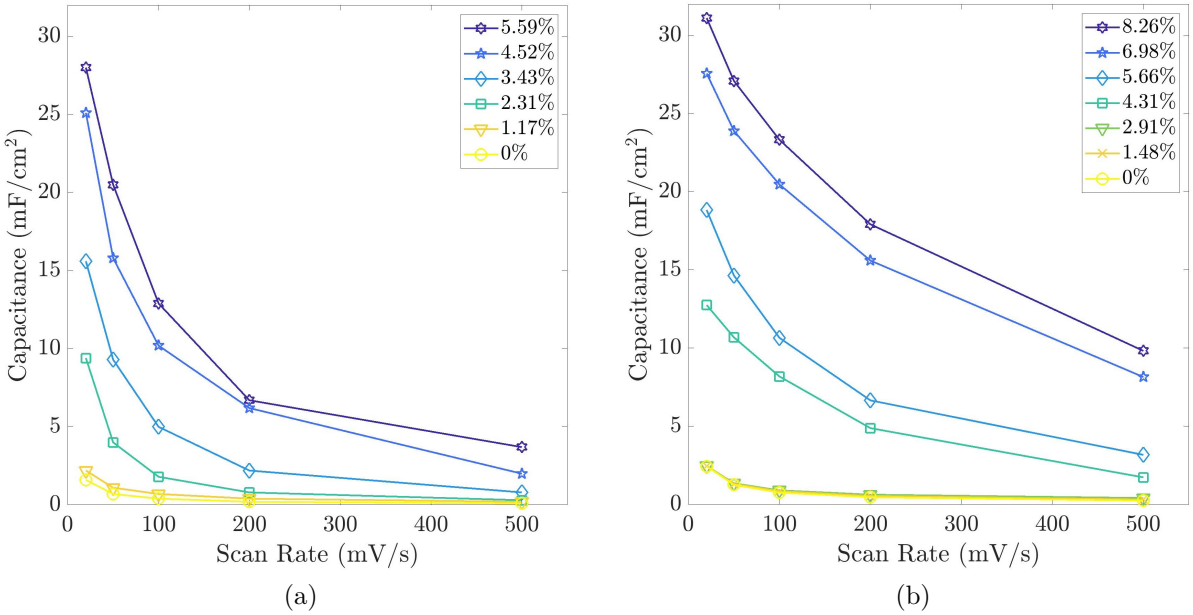

Figure 3.8: Capacitance values at different scan rates for two series of PBX at w/c of 0.42 (a) and 0.6 (b). Tests performed at an average sample age of 60 days.

observations made in Figure 3.4. For both w/c values the capacitance is increasing with increasing carbon concentration. Moreover, we can define the "capacitance percolation point": the carbon concentration threshold that triggers an increase of capacitance values with increasing carbon concentration. Its value for PBX 0.42 also corresponds to the electronic percolation point in Figure 3.6(b). We notice that capacitance values also shift with w/c: for increasing w/c, we have higher capacitance values at same scan rates. However, it is worth noting that at w/c = 0.42, for lower scan rates of 50 and 20 mV/s, we have a very dramatic increase in capacitance values versus the values at 500 mV/s. This effect is not as pronounced at w/c = 0.6 and this can make us speculate about

the causes of this difference. It might be that the cement matrix of cement/PBX samples at w/c = 0.42 is more dense than that of samples of cement/PBX w/c = 0.6, thus it is more difficult for ions to move through a dense electrode than a more porous one. This could explain why cement samples containing PBX w/c = 0.6 has much higher capacitance values at higher scan rates, but also why the values close in at lower scan rates: with a more gradual change of potential the ions have more time to move through the electrode.

3.4 Additives

Cement industry has a long history of adding different additives to cement in order to influence its properties. Supplementary cementing materials are materials that can be used alongside ordinary Portland cement. When properly used, they can improve cohesiveness, enhance workability, reduce temperature development, achieve improved strength, reduce permeability, and increase durability [57]. We have studied the possibility of adding additives to our mix in order to change its properties. In this section we will study the way cellulose, a potassium sulfate salt and a superplasticizer influenced our results.

Carboxymethyl Cellulose (CMC) is a hydrophilic organic polymer. When dissolved in water, cellulose forms a highly connected network, due to hydrogen bonds and Van der Waals interactions [58]. A water solution containing cellulose becomes more viscous with an increasing amount of cellulose dissolved. There are already numerous studies linking cellulose additives to an increase in concrete strength [59, 60, 61]. Cement is also a hydrophilic material, while carbon black is a hydrophobic, thus it does not mix with the cement paste easily. In order to improve our carbon dispersion, we considered cellulose to be a good matrix for carbon black dispersing. We synthesized cement samples containing cyclomethyl cellulose (CMC) and compared them with samples without cellulose. We used three types of cellulose: CMC 90K, CMC 250K and CMC 700K, where 90K, 250K and 700K represent the average molecular weight of the crystallized polymer (K for Kilo), which is an indicator of polymer chain length. To synthesize these samples we used 1.4% of cellulose out of total water weight and followed the protocol described in the Synthesis section (cf. §2.1).

In Figure 3.9(a) we see a comparison of resistivity values between cement/PBX composites without CMC or with CMC 250K. Samples containing cellulose have resistivities ranging from one to two orders of magnitude higher than samples without cellulose at the same carbon content. When comparing capacitance values of samples without CMC and samples with the three studied CMC molar weights in Figure 3.9(b), we can state that at this concentration, cellulose has a negative impact on our samples' electrical performance, with five or more times lower capacitances for cellulose samples. While cellulose seems to be doing a good job at dispersing carbon black, we suspect that it prevents it from establishing an adequate percolated network. This confinement of carbon black might not only play a role in the resistivity, but also in capacitance, as it would prevent the ions from successfully reaching the carbon pores, greatly diminishing the electrode's output. CMC does not seem to be a good additive for our purposes.

We started looking for ways to delay the hardening of the cement paste, which would make our paste more workable in the initial phase, thus possibly allowing the incorporation of more carbon into the mix. There have been reports since the 90's that studied mechanisms using sulfate ions in order to delay the hydration reaction and the formation of ettringite in cement [62]. Ettringite is the mineral name for calcium sulfoaluminate, which is commonly found in portland cement concretes and the formation of ettringite in fresh, plastic concrete is the mechanism that controls stiffening [63]. Thus, we attempted the use of sulfate ions and study how it affects our system. To synthesize the new samples we used the same protocol as described in Synthesis section for PBX 11%, but used a 0.14M solution of K_2SO_4 instead of water. During the mixing phase we observed a noticeable difference in the workability of the paste. This allowed us to synthesize another sample with K_2SO_4

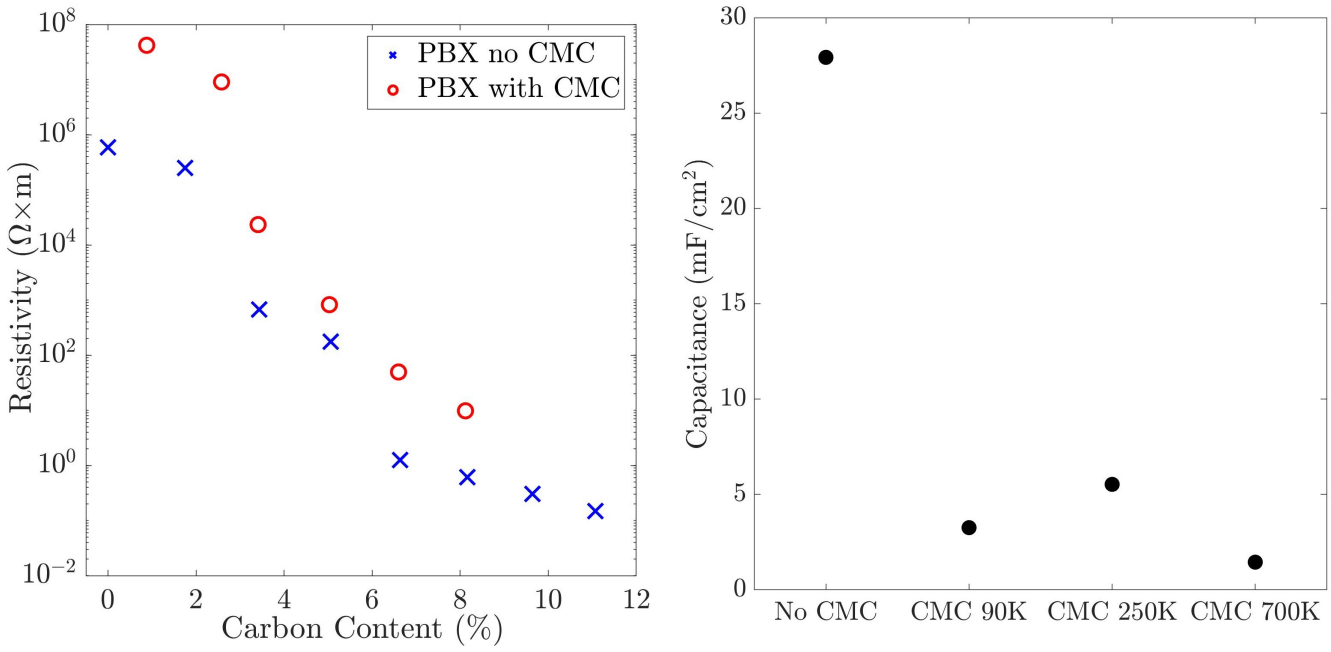

(a) (b)

Figure 3.9: (a) Resistivity vs. carbon content for two series of PBX samples with and without CMC at a molecular weight of 250K. Samples dried at 60°C over 18h. (b) Capacitance values for four samples of PBX 11% without and with three types of CMC at increasing molecular weight. Results at 100 mV/s.

and an increased amount of carbon: PBX 12.9%. We thus compared the 2 new samples with the reference sample.

As we can see in Figure 3.10(a), adding K_2SO_4 in our mix does not affect the resistivity of our samples: after taking in account the experimental error bars, the samples at 11% with and

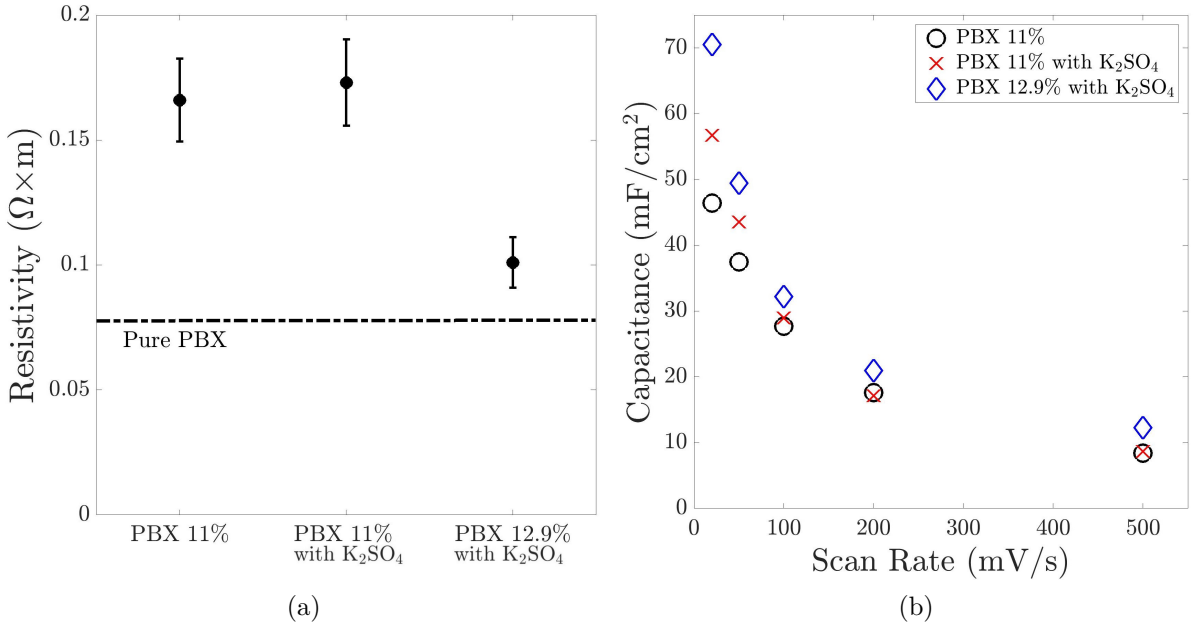

(a) (b)

Figure 3.10: Comparison of resistivity (a) and capacitance (b) at different scan rates of PBX/cement samples with and without K_2SO_4. Synthesized at w/c = 0.8. Tests performed at an average sample age of 40 days.

without K_2SO_4 are basically the same. This is an important result, that shows that influencing the kinetics of the reaction does not impact negatively the overall output. We can then see that the sample containing more carbon, as expected, has a lower resistivity, thus approaching more towards the value of pure carbon. In Figure 3.10(b) we see a comparison of the capacitance values for the same samples (as in resistivity). Overall we can say that the addition of sulfates does not affect our capacitance in a negative way, moreover, the new samples containing K_2SO_4 perform better than the reference sample, with a very noticeable difference towards lower scan rates. We could have expected the 12.9% sample to have higher capacitance values due to its higher carbon content, but it is odd to see that the 11% sample with K_2SO_4 also performs better than the reference. We can speculate that the use of K_2SO_4 effectively adds more ions to the system that can be transported and stored, thus increasing the overall capacitance.

Superplasticizers (SP) are synthetic polymers that are extensively used by the concrete industry to create high strength concrete. Otherwise known as high range water reducers, they affect the viscosity of the cement paste and greatly reduce the amount of water necessary to make the mix workable. They are also known to retard the curing of cement [64]. Superplasticizers are made from either sodium salts or calcium salts. When concrete is first mixed, the presence of water causes cement particles to be drawn to one another, which thickens the batch. Superplasticizer molecules, which are made of long chains and links, attach themselves to the cement particles and give them a highly negative charge. As a result, they repel each other. Because the cement particles are no longer attracted to the others, the concrete remains fluid [65]. While in the industry SP are used to create very dense, high performance concrete, for our applications we saw an opportunity of increasing the amount of carbon incorporated, while maintaining a good workability. The idea of using a polymer proved ineffective previously (with CMC), thus the main concern was how the use of SP would affect our current electronic properties. To study that, we synthesized a new PBX 11% sample at w/c=0.8 and used 1.6% of SP versus water weight, and we compared it to a reference sample.

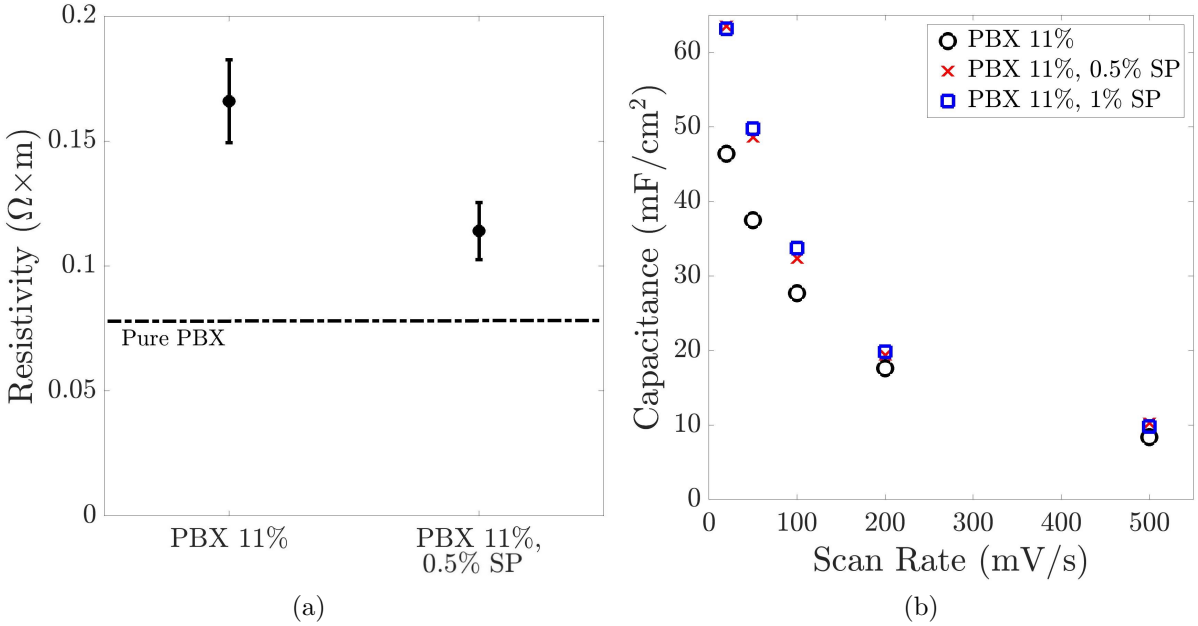

Figure 3.11: Comparison of resistivity (a) and capacitance (b) values for two cement/PBX samples at 11% wt, with and without Superplasticizer (SP). Synthesized at w/c = 0.8. Tests performed at an average sample age of 40 days.

In Figure 3.11 we can compare the resistivity and capacitance results of this new sample. We see that the resistivity of the sample containing SP is lower, while its capacitance results are

higher than the reference, with significant differences at lower scan rates. This result makes us wonder of the mechanisms involved. It is possible that due to its increased workability and retarded hydration, the carbon is better dispersed, as in the case of K_2SO_4, thus forming a more connected percolated network. However, we know that this effect of the SP is only temporary. The cement particles, though repulsed by one another, slowly become hydrated as they react with the water in the concrete. This process causes crystals made of calcium hydroxide and calcium silicate hydrate to form on the round surface of the cement. The crystals slowly engulf the superplasticizers so that they are no longer able to function. Without the negative charge to keep the cement particles apart, the concrete thickens again [65]. It is also possible that just as with K_2SO_4, there could be an ionic contribution from the SP, which would explain the spike in capacitance. However, it is important to point out that the type of superplasticizer we used belongs to the family of carboxylate superplasticizers. Different classes of superplasticizers could have different effects on the electrical properties. Overall, what we should take from this is that carboxylate superplasticizers do not affect our mixes in a negative way, thus being very promising additives that could allow the increase of the amount of carbon incorporated into the cement.

3.5 Literature comparison

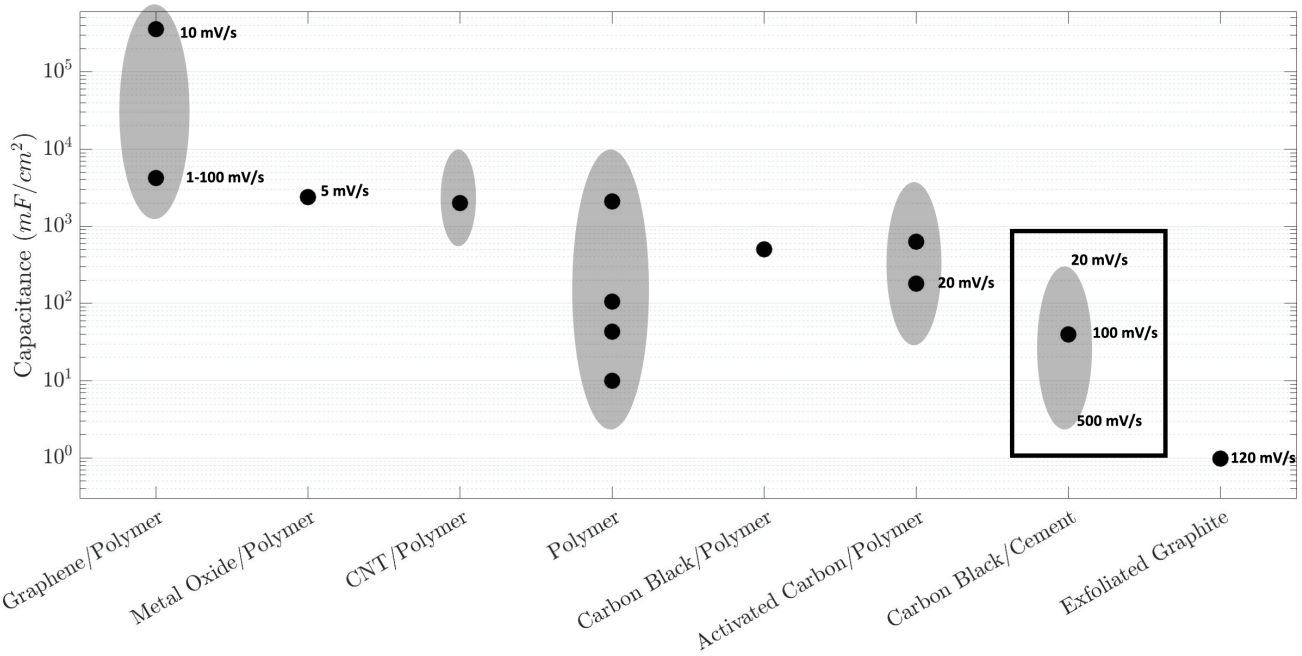

Figure 3.12: Literature comparison of supercapacitor performance for different systems. On the Y-axis, the capacitance, on a logarithmic scale, is represented in mF/cm^2 and on the X-axis - different supercapacitor systems. The black dots represent exact values found in literature and the grey areas - the capacitance range the specific systems can reach. The values next to the dots represent the scan rates in mV/s at which these results have been obtained. [66, 67, 68, 69, 70, 71, 72, 73, 74, 75].

After defining and explaining all the parameters that play a role in our samples' performance, we must not forget that our study was first of all one of exploration and optimization. It is important to step back and examine how our samples perform compared to other devices described in literature.

In Figure 3.12 we compare the capacitance values that we have obtained with our samples with a spectrum of similar supercapacitor devices. The graph is made in a log scale, spanning from a few hundreds of F/cm^2 to a few mF/cm^2, and represents different types of devices, that

use different materials as matrix, core storage and electrolyte. First of all, it is worth noting that most systems involve polymers and/or carbon under some form. Indeed, carbon nanomaterials, in particular carbon nanotubes, graphene, mesoporous carbon and carbon blacks have been widely investigated as efficient electrode materials in supercapacitors [76]. Graphene is one of the material with most potential, which can allow devices with capacitances going up to 100 F/cm^2, as well as good performance at high scan rates. Other notable devices are those using metal oxides, in particular MnO_2, that can reach capacitances of a few F/cm^2. Our own carbon black/cement system performs decently well compared to the others, with values ranging from 10 to below 100 mF/cm^2. It is a very impressive value, considering the fact that our devices are multifunctional, playing a structural role in addition of storage. In addition to that, carbon black is significantly cheaper than carbon nanotubes. It is worth noticing that most of other system are designed as electrodes for small to medium size devices, while on the other hand, our system is not limited by these dimensions. Our final application envisions potentially tens of square meters of effective surface in houses and buildings, thus allowing us to reach important storage values very quickly.

Chapter 4

Conclusion

Throughout the 9.5 months of this internship we studied the behaviour of electrically conductive cement, its important parameters, we established the measuring protocols, we designed the measuring setups and we greatly optimized the obtained results.

First, we managed to successfully mix hydrophobic carbon black and hydrophilic cement powder in order to obtain an electronically conductive carbon-cement composite. We established and refined a successful scientific protocol for sample synthesis and preparation, as well as for resistivity and capacitance measurements. We designed a measuring setup that minimizes the variable parameters involved in the measurements and reproduces the same conditions at each measurement. In addition to that, we determined the errors that must be taken into account when dealing with such a heterogeneous system.

Secondly, in terms of results, we studied the morphology and resistive properties of bulk carbon black in order to determine their resistivity thresholds. We saw that Acetylene Black, PBX and Vulcan are the least resistive types of carbon we studied, with resistivities of 34, 79 and 124 mΩ.m respectively. We determined that when mixed with cement, only AB and PBX would give us promising results: their resistivities would greatly approach those of the bulk carbon values, 80 mΩ.m for AB and 200 mΩ.m for PBX; all the while their capacitance would reach values of 32 and 28 mF/cm^2 for AB and PBX respectively. Although the type of the carbon we chose for the composite plays a crucial role in the outcome of our measurements, it is not the only important parameter. The water to cement ration (w/c) is a key parameter, since it governs the porosity of the cement samples. The carbon concentration in our samples affects the resistivity and capacitance results, which is explained by the presence of a carbon percolation point in our cement matrix. In synergy with the w/c, it creates a trend where the electronic percolation point shifts towards higher concentrations when the w/c is increasing. These thresholds show us which carbon concentrations we have to reach in order to obtained measurable electronic effects. In addition to that, we discovered that additives like sulfate salts or superplasticizers can beneficially impact our resistivity and capacitance results and even allow us to incorporate more carbon into the mix. This can open the way for some new research and new optimizations that can be made to the composite samples.

Globally, these results are meant to prove the concept and open new possibilities. The next step constitutes the upscaling of the samples in order to prove that our idea works on bigger scales. Applying the gathered knowledge on mortars and concrete and reproducing the results on samples one or two orders of magnitude bigger will certainly involve various engineering problems and redesigning of scientific protocols. In addition to that, experimenting with various other carbon types as well as exploring parameters like the electrolyte concentration are still areas worth spending time on, and they can potentially lead to further optimizations. In either case, this study will constitute a pillar on which further research can rely in order to speed up the progress.

Annex

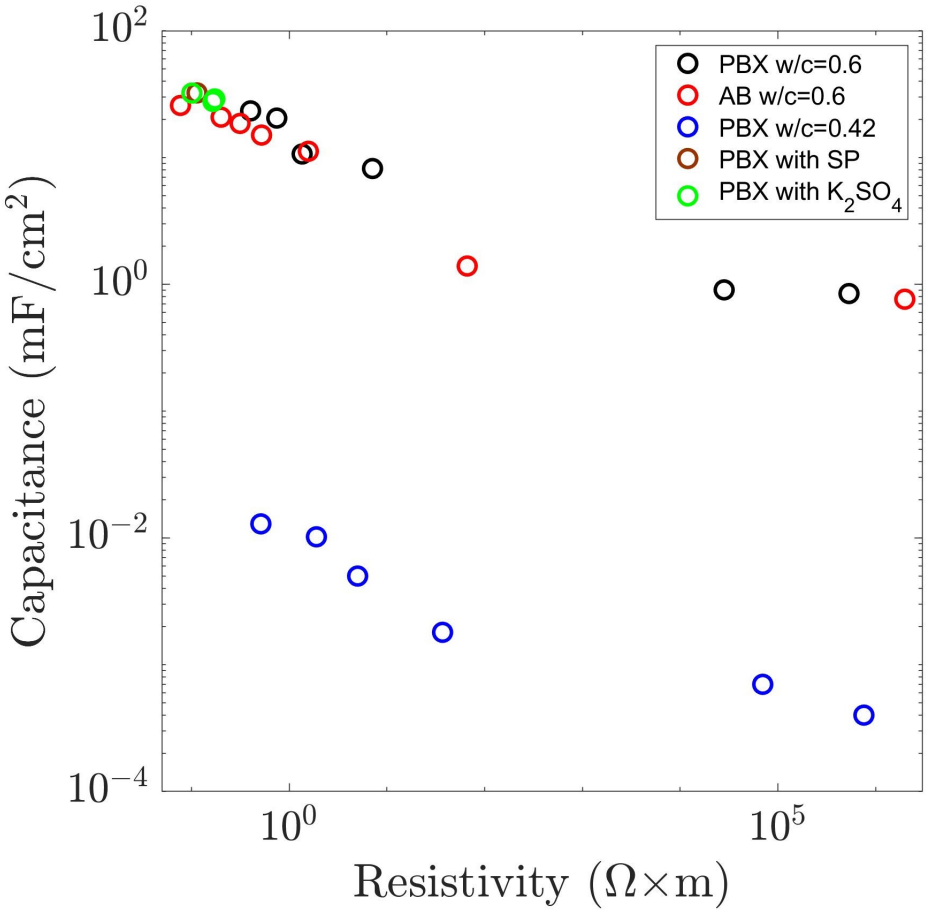

Figure 4.1: Capacitance vs. resistivity for all samples reported in this document. Cement/PBX samples containing additives have a w/c = 0.8. We see that samples having w/c = 0.6 and 0.8 are grouped together, while the series having w/c = 0.42 is shifted to lower capacitance values. Water to cement ratio, the number and size of pores have a significant effect on capacitance performance of samples.

Bibliography

[1] A. Hasanbeigi, L. Price, and E. Lin, "Emerging energy-efficiency and co2 emission-reduction technologies for cement and concrete production: A technical review," *Renewable and Sustainable Energy Reviews*, vol. 16, no. 8, pp. 6220–6238, 2012.

[2] "The cement sustainability initiative: Our agenda for action," *World Business Council for Sustainable Development*, p. 20, 2002.

[3] J. Lehne and F. Preston, "Making concrete change: Innovation in low-carbon cement and concrete," *Chatham House Report, Energy Enivronment and Resources Department: London, UK*, 2018.

[4] M. A. Nisbet, M. G. VanGeem, J. Gajda, and M. Marceau, "Environmental life cycle inventory of portland cement concrete," *PCA R&D Serial*, no. 2137a, 2000.

[5] N. Mahasenan, S. Smith, and K. Humphreys, "The cement industry and global climate change: current and potential future cement industry co2 emissions," in *Greenhouse Gas Control Technologies-6th International Conference*, pp. 995–1000, Elsevier, 2003.

[6] P. Hewlett and M. Liska, *Lea's chemistry of cement and concrete*. Butterworth-Heinemann, 2019.

[7] "https://www.understanding-cement.com/kiln.html,"

[8] H. F. Taylor, *Cement chemistry*. Thomas Telford, 1997.

[9] K. Ioannidou, K. J. Krakowiak, M. Bauchy, C. G. Hoover, E. Masoero, S. Yip, F.-J. Ulm, P. Levitz, R. J.-M. Pellenq, and E. Del Gado, "Mesoscale texture of cement hydrates," *Proceedings of the National Academy of Sciences*, vol. 113, no. 8, pp. 2029–2034, 2016.

[10] V. Grenard, *Structuration et fluidification de gels de noir de carbone*. PhD thesis, Lyon, École normale supérieure, 2012.

[11] X. Li and B. Wei, "Supercapacitors based on nanostructured carbon," *Nano Energy*, vol. 2, no. 2, pp. 159–173, 2013.

[12] M. Winter and R. J. Brodd, "What are batteries, fuel cells, and supercapacitors?," 2004.

[13] P. R. Bueno, "Nanoscale origins of super-capacitance phenomena," *Journal of Power Sources*, vol. 414, pp. 420–434, 2019.

[14] H. Whittington, J. McCarter, and M. Forde, "The conduction of electricity through concrete," *Magazine of concrete research*, vol. 33, no. 114, pp. 48–60, 1981.

[15] R. G. McCormack, "Method of making concrete electrically conductive for electromagnetic shielding purposes," Sept. 13 1994. US Patent 5,346,547.

[16] N. Banthia, S. Djeridane, and M. Pigeon, "Electrical resistivity of carbon and steel micro-fiber reinforced cements," *Cement and Concrete Research*, vol. 22, no. 5, pp. 804–814, 1992.

[17] J. Farrar, "Electrically conductive concrete," *GEC Journal of Science and Technology*, vol. 45, no. 1, 1978.

[18] J.-M. Chiou, Q. Zheng, and D. Chung, "Electromagnetic interference shielding by carbon fibre reinforced cement," *Composites*, vol. 20, no. 4, pp. 379–381, 1989.

[19] C. Association, *CAJ Proceedings of Cement and Concrete: No. 55(2001).* No. 43, Cement Association, 1989.

[20] P. Xie, P. Gu, and J. J. Beaudoin, "Electrical percolation phenomena in cement composites containing conductive fibres," *Journal of Materials Science*, vol. 31, no. 15, pp. 4093–4097, 1996.

[21] P. J. Tumidajski, "Electrical conductivity of portland cement mortars," *Cement and Concrete Research*, vol. 26, no. 4, pp. 529–534, 1996.

[22] M. S. Konsta-Gdoutos, Z. S. Metaxa, and S. P. Shah, "Highly dispersed carbon nanotube reinforced cement based materials," *Cement and Concrete Research*, vol. 40, no. 7, pp. 1052–1059, 2010.

[23] G. Constantinides and F.-J. Ulm, "The nanogranular nature of c–s–h," *Journal of the Mechanics and Physics of Solids*, vol. 55, no. 1, pp. 64–90, 2007.

[24] S. Wen and D. Chung, "Partial replacement of carbon fiber by carbon black in multifunctional cement–matrix composites," *Carbon*, vol. 45, no. 3, pp. 505–513, 2007.

[25] A. Sassani, A. Arabzadeh, H. Ceylan, S. Kim, S. S. Sadati, K. Gopalakrishnan, P. C. Taylor, and H. Abdualla, "Carbon fiber-based electrically conductive concrete for salt-free deicing of pavements," *Journal of cleaner production*, vol. 203, pp. 799–809, 2018.

[26] H. Kim, I. W. Nam, and H.-K. Lee, "Enhanced effect of carbon nanotube on mechanical and electrical properties of cement composites by incorporation of silica fume," *Composite Structures*, vol. 107, pp. 60–69, 2014.

[27] P. Genoud, "Superconductive cements," *MIT, ESPCI*, 2018.

[28] T. C. Powers, "A discussion of cement hydration in relation to the curing of concrete," in *Highway Research Board Proceedings*, vol. 27, 1948.

[29] D. Stokes, *Principles and practice of variable pressure/environmental scanning electron microscopy (VP-ESEM).* John Wiley & Sons, 2008.

[30] J. I. Goldstein, D. E. Newbury, J. R. Michael, N. W. Ritchie, J. H. J. Scott, and D. C. Joy, *Scanning electron microscopy and X-ray microanalysis.* Springer, 2017.

[31] E. Suzuki, "High-resolution scanning electron microscopy of immunogold-labelled cells by the use of thin plasma coating of osmium," *Journal of Microscopy*, vol. 208, no. 3, pp. 153–157, 2002.

[32] J. D. McDonald, *Electric power substations engineering.* CRC press, 2016.

[33] F. T. Brown, *Engineering system dynamics: a unified graph-centered approach.* CRC press, 2006.

[34] C. Feldman, "Temperature dependency of resistance of thin metal films," *Journal of Applied Physics*, vol. 34, no. 6, pp. 1710–1714, 1963.

[35] W. D. Greason, *Electrostatic discharge in electronics*, vol. 12. Wiley-Blackwell, 1992.

[36] H. Wang and L. Pilon, "Physical interpretation of cyclic voltammetry for measuring electric double layer capacitances," *Electrochimica Acta*, vol. 64, pp. 130–139, 2012.

[37] M. Singh and R. Vander Wal, "Nanostructure quantification of carbon blacks," *C*, vol. 5, no. 1, p. 2, 2019.

[38] R. Samson, G. W. Mulholland, and J. Gentry, "Structural analysis of soot agglomerates," *Langmuir*, vol. 3, no. 2, pp. 272–281, 1987.

[39] V. Trappe, E. Pitard, L. Ramos, A. Robert, H. Bissig, and L. Cipelletti, "Investigation of q-dependent dynamical heterogeneity in a colloidal gel by x-ray photon correlation spectroscopy," *Physical Review E*, vol. 76, no. 5, p. 051404, 2007.

[40] "http://www.carbon black.org", "Carbon black user's guide,"

[41] V. Trappe and D. Weitz, "Scaling of the viscoelasticity of weakly attractive particles," *Physical Review letters*, vol. 85, no. 2, p. 449, 2000.

[42] V. Trappe, V. Prasad, L. Cipelletti, P. Segre, and D. A. Weitz, "Jamming phase diagram for attractive particles," *Nature*, vol. 411, no. 6839, p. 772, 2001.

[43] M. Van der Waarden, "Stabilization of carbon-black dispersions in hydrocarbons," *Journal of Colloid Science*, vol. 5, no. 4, pp. 317–325, 1950.

[44] B. Y. Ho, *An experimental study on the structure-property relationship of composite fluid electrodes for use in high energy density semi-solid flow cells*. PhD thesis, Massachusetts Institute of Technology, 2011.

[45] D. M. Moore and R. C. Reynolds, *X-ray Diffraction and the Identification and Analysis of Clay Minerals*, vol. 322. Oxford university press Oxford, 1989.

[46] T. Denaro, V. Baglio, M. Girolamo, V. Antonucci, F. Matteucci, R. Ornelas, *et al.*, "Investigation of low cost carbonaceous materials for application as counter electrode in dye-sensitized solar cells," *Journal of Applied Electrochemistry*, vol. 39, no. 11, p. 2173, 2009.

[47] K. K. Aligizaki, *Pore structure of cement-based materials: testing, interpretation and requirements*. CRC Press, 2005.

[48] L. Raki, J. Beaudoin, R. Alizadeh, J. Makar, and T. Sato, "Cement and concrete nanoscience and nanotechnology," *Materials*, vol. 3, no. 2, pp. 918–942, 2010.

[49] A. Miyashiro, *Metamorphism and metamorphic belts*. Springer Science & Business Media, 2012.

[50] M. F. El-Kady and R. B. Kaner, "Scalable fabrication of high-power graphene micro-supercapacitors for flexible and on-chip energy storage," *Nature communications*, vol. 4, p. 1475, 2013.

[51] S. Wen and D. Chung, "The role of electronic and ionic conduction in the electrical conductivity of carbon fiber reinforced cement," *Carbon*, vol. 44, no. 11, pp. 2130–2138, 2006.

[52] G. Wypych, *Handbook of fillers*, vol. 92. ChemTec Pub. Toronto, 2010.

[53] S. Wen and D. Chung, "Double percolation in the electrical conduction in carbon fiber reinforced cement-based materials," *Carbon*, vol. 45, no. 2, pp. 263–267, 2007.

[54] L. Qie, W. Chen, H. Xu, X. Xiong, Y. Jiang, F. Zou, X. Hu, Y. Xin, Z. Zhang, and Y. Huang, "Synthesis of functionalized 3d hierarchical porous carbon for high-performance supercapacitors," *Energy & Environmental Science*, vol. 6, no. 8, pp. 2497–2504, 2013.

[55] Y.-Y. Kim, K.-M. Lee, J.-W. Bang, and S.-J. Kwon, "Effect of w/c ratio on durability and porosity in cement mortar with constant cement amount," *Advances in Materials Science and Engineering*, vol. 2014, 2014.

[56] S. Somayaji, *Civil engineering materials*. Prentice Hall, 2001.

[57] S. H. Kosmatka, B. Kerkhoff, W. C. Panarese, *et al.*, *Design and control of concrete mixtures*, vol. 5420. Portland Cement Association Skokie, IL, 2002.

[58] A. C. Khazraji and S. Robert, "Interaction effects between cellulose and water in nanocrystalline and amorphous regions: A novel approach using molecular modeling," *Journal of Nanomaterials*, vol. 2013, p. 44, 2013.

[59] T. Fu, R. J. Moon, P. Zavattieri, J. Youngblood, and W. J. Weiss, "Cellulose nanomaterials as additives for cementitious materials," in *Cellulose-Reinforced Nanofibre Composites*, pp. 455–482, Elsevier, 2017.

[60] M. Ardanuy Raso, J. Claramunt Blanes, R. Arévalo Peces, F. Parés Sabatés, E. Aracri, and T. Vidal Lluciá, "Nanofibrillated cellulose (nfc) as a potential reinforcement for high performance cement mortar composites," *BioResources*, vol. 7, no. 3, pp. 3883–3894, 2012.

[61] Y. Cao, P. Zavaterri, J. Youngblood, R. Moon, and J. Weiss, "The influence of cellulose nanocrystal additions on the performance of cement paste," *Cement and Concrete Composites*, vol. 56, pp. 73–83, 2015.

[62] H.-J. Kuzel, "Initial hydration reactions and mechanisms of delayed ettringite formation in portland cements," *Cement and Concrete Composites*, vol. 18, no. 3, pp. 195–203, 1996.

[63] M. Thomas, K. Folliard, T. Drimalas, and T. Ramlochan, "Diagnosing delayed ettringite formation in concrete structures," *Cement and concrete research*, vol. 38, no. 6, pp. 841–847, 2008.

[64] G. C. Bye, P. Livesey, and L. J. Struble, *Portland cement*. Published by ICE Publishing, 2011.

[65] V. S. Ramachandran, V. Malhotra, C. Jolicoeur, and N. Spiratos, *Suplerplasticizers: properties and applications in concrete*. 1998.

[66] L. L. Zhang and X. Zhao, "Carbon-based materials as supercapacitor electrodes," *Chemical Society Reviews*, vol. 38, no. 9, pp. 2520–2531, 2009.

[67] Y. Wang, Z. Shi, Y. Huang, Y. Ma, C. Wang, M. Chen, and Y. Chen, "Supercapacitor devices based on graphene materials," *The Journal of Physical Chemistry C*, vol. 113, no. 30, pp. 13103–13107, 2009.

[68] G. A. Snook, P. Kao, and A. S. Best, "Conducting-polymer-based supercapacitor devices and electrodes," *Journal of power sources*, vol. 196, no. 1, pp. 1–12, 2011.

[69] A. Balducci, W. A. Henderson, M. Mastragostino, S. Passerini, P. Simon, and F. Soavi, "Cycling stability of a hybrid activated carbon//poly (3-methylthiophene) supercapacitor with n-butyl-n-methylpyrrolidinium bis (trifluoromethanesulfonyl) imide ionic liquid as electrolyte," *Electrochimica Acta*, vol. 50, no. 11, pp. 2233–2237, 2005.

[70] E. Frackowiak, "Carbon materials for supercapacitor application," *Physical Chemistry Chemical Physics*, vol. 9, no. 15, pp. 1774–1785, 2007.

[71] H. Y. Lee and J. B. Goodenough, "Supercapacitor behavior with kcl electrolyte," *Journal of Solid State Chemistry*, vol. 144, no. 1, pp. 220–223, 1999.

[72] S. Mitra and S. Sampath, "Electrochemical capacitors based on exfoliated graphite electrodes," *Electrochemical and solid-state letters*, vol. 7, no. 9, pp. A264–A268, 2004.

[73] Y. Xu, Y. Tao, X. Zheng, H. Ma, J. Luo, F. Kang, and Q.-H. Yang, "A metal-free supercapacitor electrode material with a record high volumetric capacitance over 800 mf.cm^{-3}," *Advanced materials*, vol. 27, no. 48, pp. 8082–8087, 2015.

[74] C. Arbizzani, M. Mastragostino, and F. Soavi, "New trends in electrochemical supercapacitors," *Journal of power sources*, vol. 100, no. 1-2, pp. 164–170, 2001.

[75] A. Di Fabio, A. Giorgi, M. Mastragostino, and F. Soavi, "Carbon-poly (3-methylthiophene) hybrid supercapacitors," *Journal of The Electrochemical Society*, vol. 148, no. 8, pp. A845–A850, 2001.

[76] C.-F. Liu, Y.-C. Liu, T.-Y. Yi, and C.-C. Hu, "Carbon materials for high-voltage supercapacitors," *Carbon*, 2018.